DEVELOPMENT OF IMPACT AND COMPRESSION TEST FACILITIES FOR FRP PANELS

by

SARVESH MAHAJAN

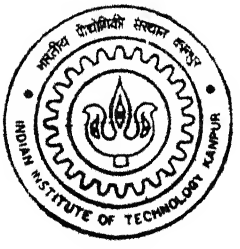

DEPARTMENT OF MECHANICAL ENGINEERING

INDIAN INSTITUTE OF TECHNOLOGY, KANPUR

April, 2001

DEVELOPMENT OF IMPACT AND COMPRESSION TEST FACILITIES FOR FRP PANELS

A Thesis Submitted
in Partial Fulfillment of the Requirements
for the Degree of

MASTER OF TECHNOLOGY

By

SARVESH MAHAJAN

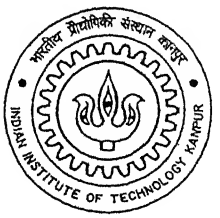

to the

Department of Mechanical Engineering

Indian Institute of Technology Kanpur

April, 2001

CERTIFICATE

It is certified that the work contained in the thesis entitled **"Development of Impact and Compression test facilities for FRP panels",** *by* **Sarvesh Mahajan,** *has been carried out under my supervision, and this work has not been submitted elsewhere for a degree.*

P Kumar

Dr. Prashant Kumar
Professor
Dept. of Mech. Engg.
I.I.T. Kanpur

April, 2001

Dedicated to

MY PARENTS

Acknowledgement

I would like to express my deep sense of gratitude to my ever-cherished guide Dr. Prashant Kumar for his invaluable guidance and help throughout my M.Tech. Programme. I am sincerely thankful for his valuable suggestions in my academic as well as personal life.

I can not forget to thank Dr. V. Raghuram for his invaluable cooperation inspite of his busy schedule. He was always there with his helping hand whenever I felt the need of his expertise. His guidance was a big supplement in making my work flawless. Working with a person, so generous, knowledgeable and down to earth is a lifetime experience for me. I would also like to thank Dr. N. N. Kishore for his time to time encouragement in completing this work.

I feel obliged to the members of ESA Lab, Mr. Divakar, Mr. Ramchandra, Mr. Anurag, Mr. B.D. Pandey, and Mr. Pankaj for helping me in various ways during my thesis and experiments.

I would like to thank my ESA lab-mates Ruchin and Sunil, who always encouraged me to deliver my best. I would also like to thank all my freinds in IIT who have made my stay here memorable. I would like to mention special thank to Mukesh, Amit, Sudheer, Tushar, Yogesh, Kumar Sarvesh, Anurag, Jaydeep, Vivek and Prakash who shared all my joys and worries during my stay in IIT.

Finally I would like to express my gratitude to my parents, brother, sister, brother-in-law, and sister-in-law who always encouraged and cooperated with me at all stages of my life.

Sarvesh Mahajan

ABSTRACT

Polymer composites are known for many attractive properties but their impact-induced resistance is poor. Impact of a foreign body affects the strength of composites considerably. Compression after impact properties becomes a critical parameter in design of structures especially in the aerospace engineering. Thus one needs to perform impact tests on the polymer composites under controlled conditions and then determine compressive strength.

An air gun test setup facility is developed for the impact test under controlled conditions. The gun is fired by the releasing high compressed nitrogen from the gas chamber of the gun. The bore of the barrel used is 12.65 mm and length of barrel is one meter. A manifold is developed to attach the pressure gauge and release valve to the gas chamber. The velocity of projectile is controlled through fine setting of nitrogen gas pressure in the gas chamber. A good quality releases valve and sensitive pressure gauge is used to maintain the pressure of gas in the gas chamber and read the pressure accurately. Projectile velocity is measured at the end of barrel using a circuit consist of laser torch, photodiode, power supply, and resistance. A digital oscilloscope is used to obtain the time pulse, which corresponds to the initial cutting of the laser beam by the front of the projectile and restoration of laser beam when the rear of projectile crosses the laser light. Accuracy in the measurement of time is in the error band of $\pm$ 0.5 μs. The design of specimen mount is an important part of this development as it is made very strong and stiff. It is designed to support a specimen of lateral dimensions of 220×150 mm. Since the mass of the projectile and its velocity are measured quite accurately the impact energy on a composite panel is known well.

Compression after impact test setup is designed to avoid buckling on the FRP panels. The impacted specimen is clamped in MTS machine for conducting the compression test on them. A buckling guide is designed to avoid buckling of a panel

during the compression test. Both halves of the guide are precision made and thick enough to be very stiff. Buckling guide is hanged on to the top frame of MTS machine symmetrically such that the specimen will not support its dead weight The strain in the direction of loading are measured by using two electrical foil type strain gauges, bonded back-to-back, of 2mm length. A specially designed virtual instrumentation is used to record the strains as well as load during the test.

The tests are conducted on two different kinds of panels having thickness of approximate 2.5mm and 3.5mm. The impact over the specimens is done with impact energy ranges from 6.0 to 6.5 Joule. The results of Compression after impact test show that the developed experimental setup works well.

List of Figures

Contents

CHAPTER 1

INTRODUCTION

1.1 INTRODUCTION

The present scenario of technological development require the new materials which can withstand the severe working and loading conditions, particularly in the field of air and ground transportation, structures, space ships, aircraft, sports goods etc. The requirement of these applications is the materials of lightweight, high strength, high toughness, and environment and corrosion resistance. The demand for such materials with versatile properties encourages the search of new materials. The single materials (aluminium, steel etc.) are losing their ground in such applications thus the composite materials comes into the picture.

Polymer composites consist of two or more phases, all phases are chemically and physically different. These materials have one or more discontinuous phases (fibers) embedded in continuous phase (matrix). The discontinuous phase is generally stronger and stiffer than continuous phase.

Polymer composites are known for their distinct properties such as high specific modulus and specific strength, fatigue and corrosion resistance. But these properties depend on the properties of constituents as well as on the behavior of interface between the fibers and matrix. Though composites have many attractive properties but their impact-induced resistance is poor. Impact of a foreign body affect the different properties of composite, tensile and compressive strength, etc. To understand the effect of impact on the composite materials one needs to conduct impact tests under controlled conditions. In some of the practical applications it is of interest to know the compressive strength of

composite after impact. These requirements are the background and motivation for the present work.

When a solid is subjected to any type of loading, static or impact, it can absorb energy by two basic mechanisms: (1) creation of new surfaces and (2) material deformation. The material deformation occurs first. If the energy supplied is large enough, a crack may initiate and propagate, thus actuating the second energy-absorbing mechanism. The material deformation continues in advance of the crack during crack propagation.

It can be assumed that failure in a fiber composite originate from small, inherent defects in the material. These defects may be broken fibers, flaws in matrix, debonded interfaces. There are several possible local failure events occurring during the fracture of a fibrous composite. At some distance ahead of the crack the fibers are intact. In the high stress region near the tip they are broken, although not necessarily along the crack plane. Immediately behind the crack tip fibers pull out of the matrix. In some composites the stress near the crack tip could cause the fibers to debond from the matrix before they break. The various mechanisms involved during crack propagation account for the total energy absorbed in the fracture process.

The most of matrix materials (i.e. epoxy) used in composites are inherently brittle in nature. Moreover, in a laminate there is no reinforcement of fibers along the thickness hence an interface is rich in matrix having very little energy absorbing capacity at the interface. It makes them vulnerable to delamination failure under impact loading. Thus the various factors that contribute to delamination of polymer composites are complex nature of induced stresses, brittle nature of constituents, poor interface bonds, difference in properties of constituent elements like modulus, complex energy absorbing mechanisms, microcracks, and material discontinuities, etc. Due to low toughness of interface in polymer composite laminates, once a delaminated crack is initiated by an impact it propagates at very high speed. As a result even a minute impact load like hailstorm, runway debris on an airstrip, drop of work tool, foreign object impact (like

bird hitting etc.), etc. causes extensive delamination around the point of impact. On the other hand, when a sheet of conventional metals is impacted by a foreign body usually it is not cracked because of local yielding. Further, the propagation of crack is inhibited owing to work hardening of metals. Therefore, impact loading causes more severe damage in composite materials as compared to conventional metals. The presence and growth of delamination crack results in the progressive reduction of stiffness and strength of composites.

In many engineering applications of composite materials high strain rate or Impact loads are expected, therefore the suitability of composites in such application is not only determined by usual design parameters but by impact properties also. Thus, it becomes important to know the impact behavior of composites for both safe and efficient design.

A very common way to evaluate impact properties is to determine the toughness of material by knowing the energy required to break a specimen of a particular geometry. The well known Charpy and Izod impact tests are very useful for comparing the impact properties of different materials. For composites the fracture phenomenon is much more complex. The mode of fracture and therefore the absorbed energy during impact are influenced by various test variables such as fiber orientation, specimen geometry, velocity of impact, etc. However, Charpy and Izod tests do not give the data of basic physical significance. The velocity of impact also can not be varied with large range in these conventional methods. This has resulted in the development of the other type of testing setups i.e. Drop-Weight impact test, Air Gun impact test setup.

1.2 LITERATURE SURVEY

The study of impact behavior of fibrous composite materials did not receive much attention until the mid-1960s. The early published results on the subject were

obtained with a standard Charpy impact machine without any attempt to study the phenomenon of impact.

In 1970s L.J. Broutman and his associates performed extensive impact studies on a specially built drop-weight impact-testing apparatus in which several experimental parameters could be easily varied. They performed their studies on glass-fiber-reinforced epoxy and polyester resin and on hybrid graphite-Kevlar-glass composites. Through high- speed photography, important observations on the phenomenon of fracture and associated energy-absorbing mechanisms were made. Experimental parameters, which were varied, included fiber orientation, velocity of impact, drop weight, and specimen dimensions. In the same era, Dorey et al. conducted the experiments to evaluate the residual tensile strength of carbon/epoxy. They also determine how the damaged area depends on projectile velocity.

Mallick and Broutman (1975) showed that in case of cross ply specimen energy of absorption was lowest at 45° orientation. Agarwal and Narang (1977) conducted a Charpy impact test on composite materials with all unidirectional fibers. Results indicate that the impact energy continuously decreases with increasing fiber orientation. Minimum impact energy is observed at 90° orientation.

Takeda et al. (1982) showed that transverse cracks are associated with delamination failure. In another study, they concluded through high speed photography that the transverse flexural and membrane tensile waves cause most of the delamination failures. Caprino (1984) observed that the main parameter for evaluating the extent of panel damage is the incident energy of the impacting projectile and not the velocity.

Liu and Malvern (1987) studied to observe the matrix cracking in glass/epoxy plates. It was observed that matrix crack in an impacted plate are a result of stress concentrations at the fiber matrix interface and are produced by tensile stress. Wyrick and Adams (1988) studied the residual properties of carbon-epoxy composite subjected to

repeated impacts and results shows the good amount of reduction in tensile and compressive strengths.

Kumar and Badri (1990) studied effect on impact damage in KFRP through replacement of surface plies with glass fabric plies. They found the reduction in impact damage after replacement of surface plies of KFRP by glass fabric plies. The laminates were impacted by a stainless steel projectile accelerated through air gun.

Kumar and Narayanan (1990) studied to evaluate the energy dissipation of projectile impacted panels of glass fabric reinforced composite. They also found that the damaged area is not depended on whether a target panel is rigidly clamped at its edges or is suspended with two threads to keep the edges traction-free. Kumar and Badri (1991) conducted an experimental study to see the impact damage on single interface GFRP laminate impacted by a steel projectile with a hemispherical nose.

Chao and Tu (1998) proposed a three-dimensional contact dynamics of laminated plates. An innovative solution method was developed for the impact contact problem by using volumetric displacements as control variables and discrete path loading as state variable.

Kumar and Singh (1999) studied the impact damage area and interlaminar toughness of FRP laminate by modifying the epoxy resin with the addition of CTBN 1300X8 and tripheylphosphine under a controlled atmosphere of inert nitrogen gas. When impacted by a steel projectile they found the significant reduction in damage area (35-55%) and increase in interlaminar energy release rate was found to be near to 41%.

Jung-Kyu Kim and Ki-Weon Kang (1999) developed a new analytical method for predicting the impact force from the dynamic strain of composite plates subjected to transverse impact. To verify this analytical method, they performed impact tests on plain-

weave glass/epoxy composite plates having various thickness. The impact forces obtained by the analytical method agree well with the experimental results.

Caprino (2000) studied for the prediction of penetration energy for fiber reinforced plastics subjected to low velocity impact. It is shown that, for a given fiber type, the penetration energy is substantially influenced by the total fiber volume and tup diameter. Adanur et al. (2000) studied the glass/epoxy composite materials for chassis frame of an automotive. They conducted the experiments on Instron Dynatup-8250 impact testing machine to study the impact properties of the glass/epoxy.

Ching C. Chao et al. (2000) has presented the three-dimensional nonlinear damage mechanics of composite. Innovative failure criterion is presented for the three-dimensional damage of the laminates including tensile and shear cracking, interlaminar delamination, brittle fracture in good agreement with experimental data.

In critical products like primary structures of aeroplanes (like wings, fuselage, etc.) made of polymer composite, compressive strength after an impact of a foreign body is found to be useful parameter by designers. Thus whenever a material modification is made in composite laminate, the designer would like to know compressive strength after impact. Since these tests are done for commercial purposes, the results are hardly published in literature (Mangalgiri, 2000, ADA, Bangalore).

1.3 PROBLEM DEFINITION

The basic problem is to evaluate the compressive strength of FRP panels. The problem consists of two parts (a) impact test of FRP composite panels and (b) compression test of impacted panel. In the present work a specially designed experimental facility is developed to evaluate the compressive strength of impacted FRP panels. An air gun impact test setup is developed for a foreign body impact on a FRP panel under controlled conditions. The velocity of projectile is the controlled parameter in test, which is regulated by using a compressed nitrogen gas in the gas chamber of the

air gun. Chapter 2 describes the development of the experimental facilities for impact test. Chapter 3 discusses the design and development of compression test facility of a FRP panel after it has been impacted. An MTS machine is used to perform the compression test on the impacted panels. The setup is design to avoid buckling during the test.

In Chapter 4 the results of a few experiments of compression after test are presented to show that the developed experimental setup works well. Chapter 5 presents the conclusion of the works and suggestions for future work.

CHAPTER 2

IMPACT TEST SETUP

2.1 INTRODUCTION

This chapter deals with the development of Impact test setup for a foreign body impact over a specimen with a low velocity. The impact that does not cause through the thickness penetration is usually termed as low velocity impact. The setup is developed so as to perform the tests under controlled condition. Velocity of the foreign body is controlled to a predetermined value and is measured accurately. Proper mounting of FRP panels was considered during the development.

In the present work an Air Gun is used to perform impact test on FRP specimen. The layout for the test setup with different parts is shown in Fig. 2.1(a). A short projectile is employed to impact the specimen. The projectile is accelerated in the barrel of air gun. Its geometry is shown in Fig. 2.1(b). A FRP specimen panel is placed such that the normal of the panel is parallel to the axis of air gun to have a normal impact of projectile on the specimen panel. Compression after impact tests was also conducted on the impacted specimens. Details of compression after impact test are described in the subsequent chapters. A photograph showing developed air gun setup is shown in Fig. 2.2.

2.2 SPECIMEN USED

Polymer composite panels are employed for the impact test in this study. The panels are made from fabric based glass fiber reinforced polymer composite.

This section deals with the specimen geometry, raw materials used, preparation of preforms, their cross section, laminate preparation from the preforms, and specimen preparation from laminates.

2.2.1 Dimensions

The dimensions of the specimen used are as per shown in Fig. 2.3(a) and as follows:

Length	220 mm
Width	150 mm
Thickness	2.0 – 4.0 mm

2.2.2 Specimen Preparation

The two basic materials are being used for the preparation of specimen, glassfiber fabric and matrix (epoxy resin mixture).

The glassfiber fabric used is purchased from Harshdeep Industries, Ahemdabad. Its specifications are as follows:

Number of yarns per 25 mm in warp	= 40
Number of yarns per 25 mm in weft	= 36
Area Density	= 146 gm/m^2
Width of cloth	= 150 mm.

The matrix consists of epoxy LY-556 and hardener HT976 (4,4 – Diaminodiphenyl Sulphone) along with accelerator XY73 (used for proper curing of epoxy) and silane (used for good wetting of fibers) in the weight ratio of 100:35:1.5:0.5. Epoxy, accelerator, and silane are purchased from Ciba-Geigy Ltd. Bombay and hardener HT976 is purchased from Advanced Formulated Compounds, Atlanta U.S.A. Specimen preparation starts with the making of prepreg tapes. Prepreg tapes are prepared on a Unidirectional Prepreg Machine, developed by Kumar et al. (1995). The prepregs are made at 95°C and stored at -18°C.

Two different types of specimens are prepared to test. One is made of 20 layers and other is made of 28 layers. Usually 8 layers of prepreg tapes give 1mm thickness to the specimen.

For making a specimen plate a preform is prepared from the prepregs. The cross section of preform is shown in Fig. 2.3(b). The prepregs are cut to an approximate length of 240 mm and the layers of the prepregs are then stacked on a glass fiber reinforced Teflon sheet (GFT sheet). The prepregs oriented to have warp of all plies in one direction Another GFT sheet is placed over the stack of the prepregs. GFT sheets are perforated with 1-mm diameter holes at 10-mm apart in both the directions to facilitate the flowing out the extra epoxy and air bubbles during the curing of preform. Then the stack with these two GFT sheets is placed between two-breather sheets. These breather sheets are made of woolen blanket. The woolen blanket used in the present work has an area density approximately equal to 360 gm/m^2 and has been purchased locally. The entire set is then sandwiched between another set of GFT sheets (these sheets do not have any holes). These sheets protect the platens of press from the epoxy coming out during the curing.

Now the preform is placed in between the platens of a hydraulic press to prepare the laminate. The fixture used for laminate preparation is shown in Fig. 2.3(c). To cure the preform pressure and temperature are applied by platens of hydraulic press. The curing cycle is completed in three steps. First of all, the temperature is increased to 120°C and maintained for one hour. During this phase pressure is not applied. In second step pressure is slowly increased to 0.7 MPa and the specimen is kept upto one hour on this pressure and temperature of 120°C. For post curing, the same pressure is maintained and temperature is increased to 150°C and this state is maintained for next one hour. Then, the laminate is cooled slowly upto room temperature and is taken out from the hydraulic press.

To achieve the proper dimensions of the specimen from the laminate, it is marked according to required dimensions and trimmed by using a diamond cutter.

2.3 AIR GUN

The Schematic diagram of Air Gun Impact Set up is shown in Fig. 2.1(a) and a photograph showing the developed setup is shown in Fig. 2.2. This section will describe all the components and their functions one by one.

The air gas chamber is made of stainless steel and stores the compressed Nitrogen gas at a predetermined pressure. It is attached to the airgun barrel through a solenoid valve. The nitrogen gas in the gas chamber is fed from a gas cylinder filled of Nitrogen. The barrel was made in Gun Factory, Kanpur with the bore dimension of 12.65 mm; the barrel is one meter long having its outside diameter 25 mm.

One needs to measure the pressure of gas chamber and control it to a desired level. This led to the development of a manifold to be attached to the gas chamber. To the manifold a pressure gauge is attached to measure the pressure of gas chamber accurately. A release valve is used to release the extra gas from the gas chamber. Design and dimensions of the arrangement is shown in Fig. 2.4. It is worth noting that the manifold is designed to have minimum number of parts in the air pressure line and instead of using tubes to join various components, a solid mild steel block is used with internal holes. A photograph of manifold assembly with gas chamber is shown in Fig. 2.5.

The solenoid valve is one of the important parts of the setup. It is a kind of isolation valve, which can substitute traditional gate valves, ball valves, and butterfly valves. It is used where it becomes difficult to control the gate opening or the accuracy becomes a priority. It is an electromechanical device that utilizes a solenoid coil to control the opening and closing of the valve. Electrical current supplied to the coil creates a magnetic field, which in turn open the valve orifice. Valve position is directly proportional to the applied current.

The specifications of solenoid valve used are:

TYPE:	IMVD-10
VOLTS:	230 VOLTS
C/S:	50
WATT:	8
MAX. TEMP. :	100 °C
MAX. PRESSURE:	14 – 17 atmospheric
ORIFICE SIZE:	10 mm

A solenoid valve is superior to other valves because:

- It can be opened easily and quickly as only an electric switch operates it.
- It is very convenient as it can directly be mount on the line of flow and it comes as a single component.
- A full opening is assured.
- It is simpler in construction.

A bottom mild steel channel is used to mount the parts of air gun. The dimensions of channel to be purchased are as follows:

Width	200 mm
Height	75 mm
Length	5 m
Wall thickness	8 mm.

Two supporting stands are used to support the barrel of air gun. The stands are mounted on the bottom channel.

The gas chamber is not bolted to the bottom channel so that it can slide back and forth during recoiling. However, it is supported on both sides with suitably designed supporting angles as shown in Fig. 2.6.

2.4 SPECIMEN MOUNT

A good supporting facility is required to hold the specimen during the impact. The requirement for the supporting plates are that they should not deform during the impact, the clamping should also not be loosen during the test, and both surfaces of a specimen, front and rear, should be clamped.

The specimen mount is already shown in Fig. 2.1. The specimen mounting arrangement was developed in three parts, rear base frame, rear mount plate and front mount plate. Assembly of mounting arrangement is shown in Fig 2.7.

The rear mount plate, as shown if Fig. 2.8(a), is made from a rigid mild steel plate of 22-mm thickness. A wide groove of 1.7-mm depth and 150-mm width is cut in the plate so that a specimen can be slided into the groove. A rectangular frame shown in Fig. 2.8(b) of 200mmX175mm external dimensions and 125-mm square hole is used to clamp the specimen on the rear mount plate with the help of eight M10 capscrews as shown in Fig. 2.9. Both rear and front mount plates have the sufficient thickness to resist any deformation in it during the test. The surfaces of the plates, which are in contact with specimen, are machined properly so that they do not scratch the specimen surfaces.

The rear mount is screwed to the rear base frame with four M10 screws. The rear base frame is designed to be very stiff and strong with the help of 10mm thick webs as shown in Fig. 2.10. The developed specimen mount assembly mounted on the bottom frame is shown in Fig. 2.11.

2.5 VELOCITY MEASUREMENT SYSTEM

Suppose one knows the distance, L, between two points A and B. If a body crosses this length in time t then its velocity is L/t. Similarly one can state another concept. If a body of length L crosses the point A in time t, its velocity is L/t.

In the present work second concept is used The velocity of projectile is measured at the moment when it comes out from the Gun Barrel. A laser torch is used to generate the laser beam (one can assume it a point light) and the beam is fallen on a photodiode. The photodiode is connected to an oscilloscope through a circuit as discussed later in the section. The laser beam is centrally aligned to the center of barrel. As the light of laser beam falls on to the photodiode a line of 5 volts is obtained on the screen of oscilloscope. When projectile cuts the laser beam voltage drops to zero in the circuit connected to the photodiode and the oscilloscope shows zero voltage during that period Thus the oscilloscope displays a pulse as shown in Fig. 2.12. From the pulse the time of travel (t) of projectile is evaluated. Knowing the length of projectile L, the velocity of projectile is L/t. The line diagram including the laser torch and photodiode is shown in Fig. 2.13. A photograph of laser torch and photodiode inline with the gun barrel is shown in Fig. 2.14.

2.5.1 Circuit Diagram Used

The circuit diagram through which the photodiode is connected to the oscilloscope is shown in Fig. 2.15. The photodiode is connected in reverse biased mode with the power supply of 5 Volts. In the reverse biased mode initially the photodiode has a very high resistance and no current flows through the circuit. As the laser beam light falls on the diode a conduction path is generated which decreases the resistance of diode close to zero and current starts to flow. A voltage equals to the voltage of power supply comes across the point A and B as shown in Fig. 2.15. Thus, the initial setting corresponds to the laser light falling on the photodiode with 5V input to the oscilloscope. As the front of the projectile cuts the laser beam the voltage drops to zero but it is

recovered again when the rear face of the projectile passes the laser beam. There are rise and fall times of the pulse thus obtained. However, initiation of rise and fall are taken to be the representative values and they can be read with an accuracy of $\pm$ 0.5 μs.

2.5.2 Arrangement of holding the Laser Torch and Photodiode

The velocity measurement system adopted in the present work is required to hold, adjust and align the laser torch and the photodiode. The holding arrangement used for laser torch has the motion in two directions (horizontal as well as vertical) and for photodiode it has motions in both X and Y directions and rotations as well.

An X-Y verneer alignment system (can be seen in Fig. 2.11), used in an optical microscope to align a specimen, is employed to hold the laser torch. It is mounted vertically to the bottom channel of the air gun system such that the laser beam can be moved up and down and horizontally parallel to the axis of the barrel. A suitable holding block is designed to hold the laser torch and is attached to the X-Y alignment system. The design and dimensions of the block to hold laser torch are shown in Fig. 2.16. The holding block is attached to the X-Y alignment system with the help of two M6 screws. The laser torch is clamped to the mount block with the help of two M4 screws. A M6 screw is used to press the "on button" of the laser gun, whenever the laser light is required. The torch holding block with X-Y verneer mounted on alignment system can be seen in Fig. 2.14.

The photodiode is mounted on the stand as shown in Fig. 2.17. Photodiode is stacked over a Bakelite block (as shown in Fig. 2.14), which is mounted on a plate A with the help of screw B. The plate A is integrated with rod C which is mounted on rod F (integrated with base plate) through a hollow circular cylinder D. Screw B allows the diode to be move in the direction parallel to the axis of barrel over plate A. The block D is allowed the vertical motion and rotations as well with the help of screw E. This provide all required motions to the photodiode.

The laser beam is initially set to coincide with the rim of the gun barrel and later it is centered to the axis of the barrel by moving the torch arrangement with the X-Y alignment system. Thereafter, the photodiode mounted on a stand is aligned to the laser beam.

2.5.3 Measurement of Velocity and Energy of Projectile

The velocity of projectile is measured by having a voltage pulse on the screen of digital oscilloscope as shown in the Fig. 2.12. The data is transferred to a personal computer using GPIB software. The data analyzed by the computer is then plot by using the GNUPLOT software. Then, on the plot one can elaborate the points of interest to measure the time of flight for projectile upto the accuracy of $\pm$ 0.5 μs.

To find the projectile velocity and energy, all the three quantities i.e. mass, length of projectile and time duration are measured very accurately. The error analysis (Appendix "A1") shows the error band to be $\pm$ 0.5% for a typical measurement of the study.

2.6 EXPERIMENTAL TECHNIQUE

In this study, a cylindrical projectile is used to impact the laminates. The length of projectile used is 22 mm (approximate) and diameter is 12.6 mm. The projectile is made of mild steel and weighs 7.55 gm. The low mass (<10 gms) of projectile is required because impact with very low impact energy is planned for in this study. Then the mass of projectile should be low to have a reasonably high projectile velocity. It is to be noted that for a very low velocity, projectile would drop considerably between the exit end of the barrel and the FRP impact plane, which is placed 300 mm away. It is estimated (Appendix"A2") that projectile goes down by only 0.5 mm with a velocity of 30 m/s.

The laminate is rigidly fixed in the mountings described in Sec. 2.4. The projectile is accelerated in the barrel of air gun, shown in Fig. 2.1(a), with the help of

Nitrogen gas accumulated in the gas chamber. The Solenoid Valve is used to release the gas of the gas chamber. The velocity of projectile is calibrated with respect to the pressure in gas chamber, which is measured by the pressure gauge mounted in gas chamber. The required velocity of projectile is controlled through the pressure of the gas chamber. The release valve mounted with pressure gauge to the gas chamber is used to control the pressure of the gas chamber. The specimen mount is positioned such that the projectile hits the specimen in the center.

2.7 ESTIMATION OF PROJECTILE VELOCITY

Velocity of projectile is estimated against the pressure of gas in gas chamber. Projectile of 8.186 gm. and 22.2 mm in length is used to calibrate the velocity against the pressure used to accelerate it. Two type of calibration curves for energy as well as velocities are shown in the present work. These are predicted and actual. The predicted one is obtained by using the principle of energy balance. If the pressure in gas chamber is P, length of barrel is L, and area of cross section of projectile is A, the force F on the projectile is $F = P \times A$ and the work done on the projectile during its acceleration in the barrel is given by $W = P \times A \times L$.

It is worth noting that the gas chamber is quite large in compression to the volume of the barrel and the reduction of pressure can be neglected during expansion of nitrogen gas in the barrel.

The kinetic energy of projectile is $E = (\frac{1}{2}) \times M \times V^2$. To estimate the projectile velocity, the friction in the barrel is neglected and the work done on the projectile is equated to its kinetic energy

$$PLA = (\frac{1}{2})\, MV^2$$

yielding,

$$V = \{(2PAL)/M\}^{1/2}$$

The predicted and experimentally measured curves for velocity and energy against pressure are given in Fig. 2.18(a) and 2.18(b). The difference between the predicted and actual curves is expected because of the assumptions, (i) the projectile moves in the barrel with zero friction and (ii) the pressure acting on the projectile remains constant.

2.8 CLOUSURE

The experimental setup has been developed successfully and numbers of tests have been carried out with the setup. The work presented in this chapter consists of description and development of setup, designs and dimensions of different parts of setup and assembling of setup. The main parts of setup are mounting arrangement for specimen, arrangement to attach the pressure gauge and release valve to the gas chamber, velocity measurement system, etc. A manifold is designed to attach the pressure gauge and release valve and attach them to gas chamber. Proper mounting arrangement is designed to clamp the specimen for test. For velocity measurement a circuit is used consisting of laser beam, photodiode, power supply, resistance and oscilloscope. A good arrangement is made to hold the laser torch and photodiode in line with the axis of gun barrel. Calibration of projectile velocity and energy with respect to pressure, using a steel projectile of 8.18gm, is also shown.

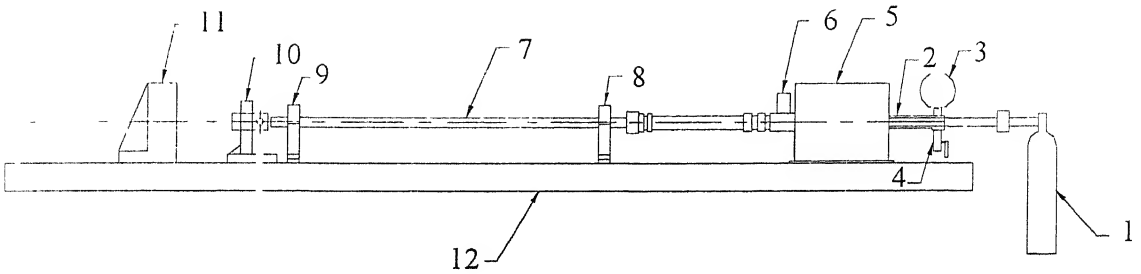

1. Air Gas Cylinder
2. Manifold to accommodate the pressure gauge and release valve
3. Pressure Gauge to measure the pressure of Gas Chamber
4. Release valve to release the extra gas of Gas Chamber
5. Gas Chamber to accumulate the gas before firing
6. Solenoid Valve to Release the Gas for firing
7. Barrel
8. Stand to hold barrel on Frame
9. Stand to hold barrel on Frame
10. Arrangement to hold the Laser torch for velocity measurement
11. Specimen Mount
12. Frame to establish the setup.

Fig 2.1(a) Schematic diagram of air gun Impact Test Setup

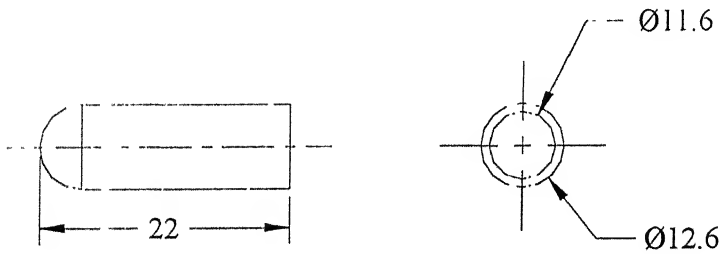

Fig. 2.1(b) Dimensions of projectile used

Fig. 2.2 A photograph showing air gun setup

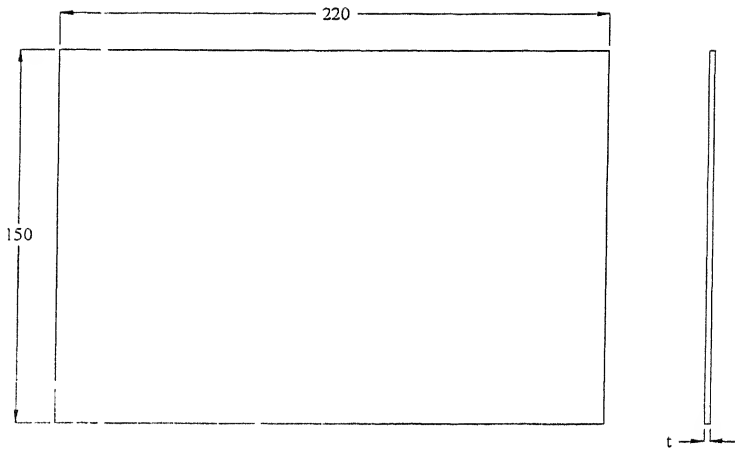

$2.0 \leq t \leq 4.0$

Fig. 2.3(a) Specimen dimensions used in the experiment

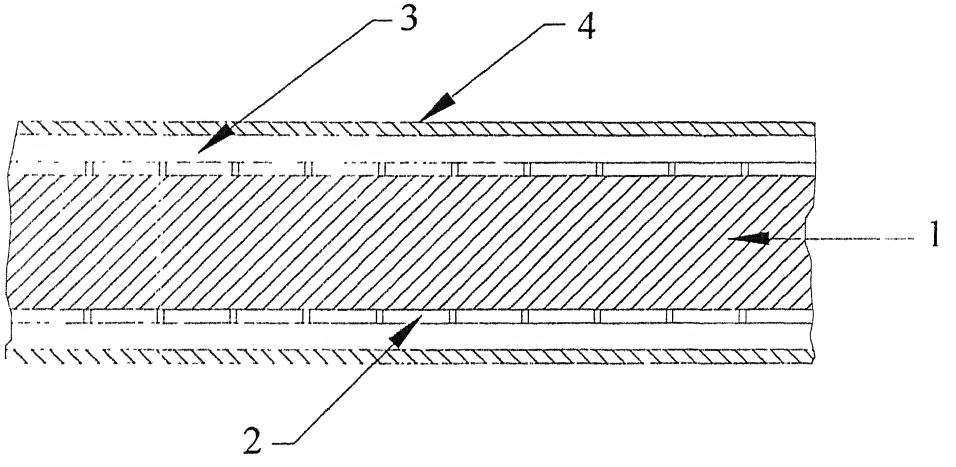

1. Stacks of prepreg layers, 2. GFT sheet with holes, 3. Breathers, 4. GFT sheets.

Fig. 2.3(b) Cross section of Preform along with Teflon sheets and breathers

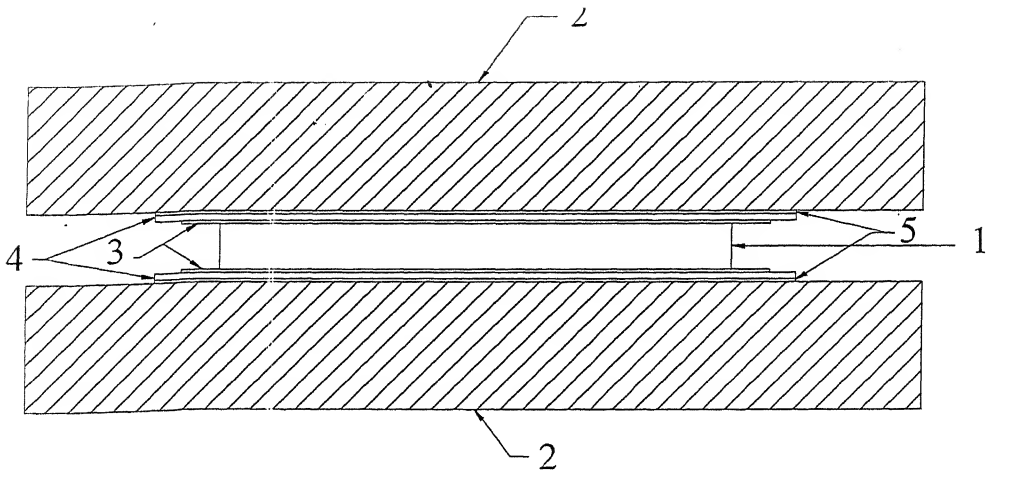

1. Laminate 2. Heated Platens of Press 3. GFT sheets with perforated holes 4. Breathers 5. GFT sheets

Fig. 2.3(c) Curing of laminate in a hydraulic press with heated platens

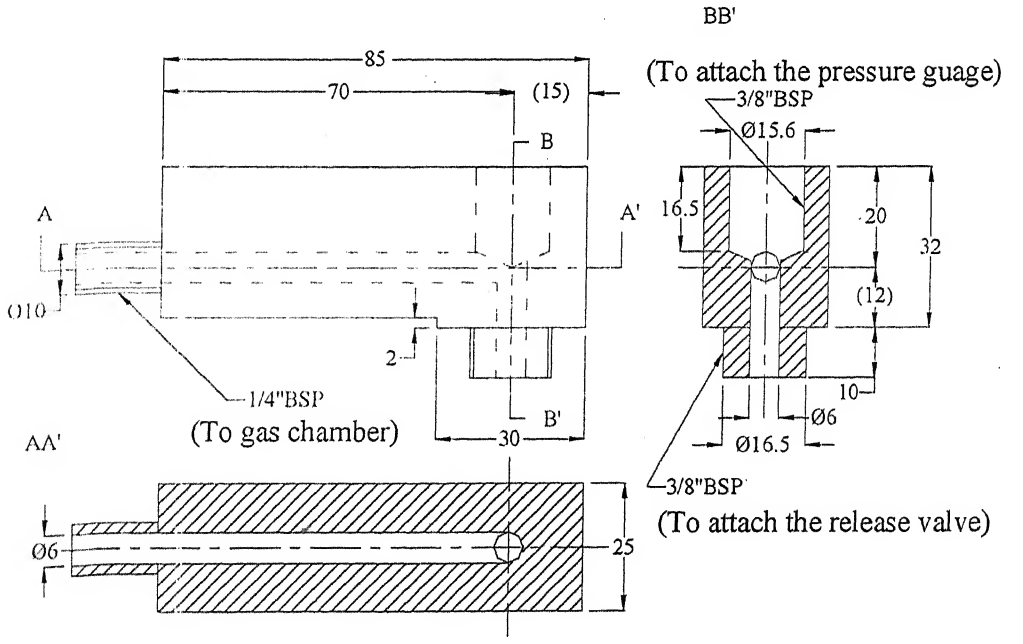

Fig. 2.4 Manifold to mount pressure gauge and release valve

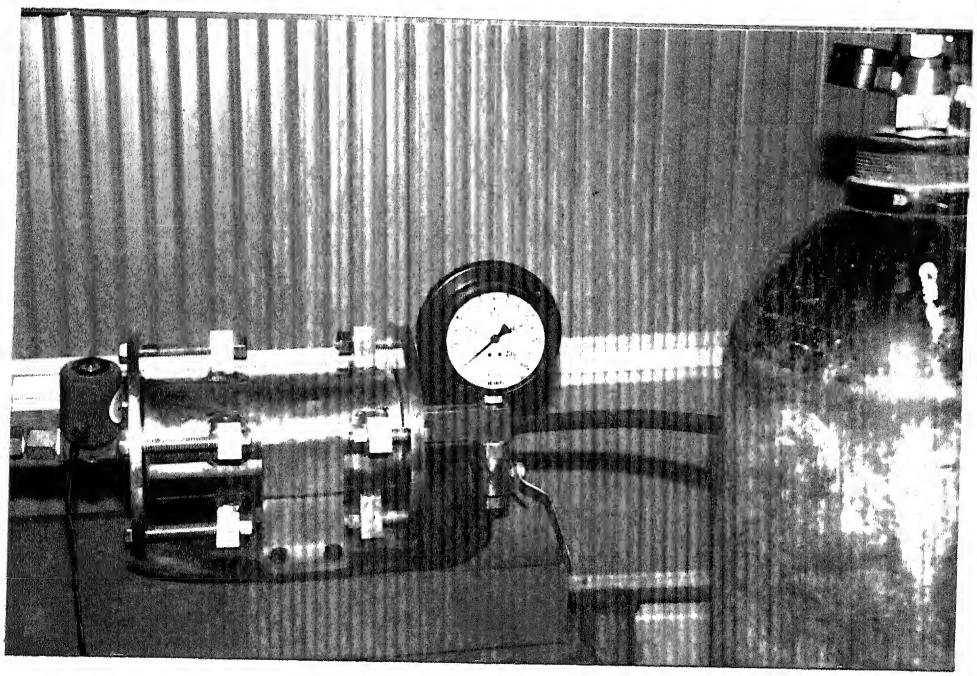

Fig. 2.5 A photograph of manifold assembly with pressure gauge, release valve and gas chamber

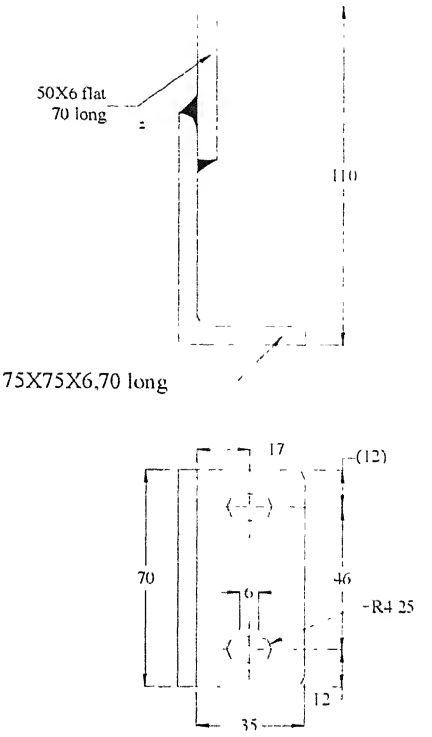

Fig. 2.6 Side supporting angle mounted on the bottom channel to support the gas chamber

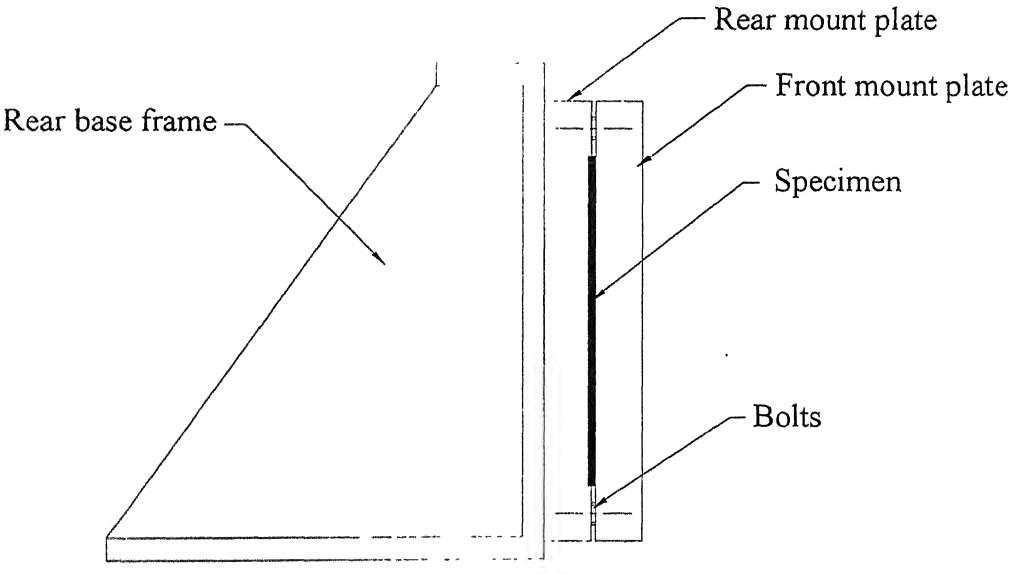

Fig. 2.7 Assembly of mounting arrangement of specimen

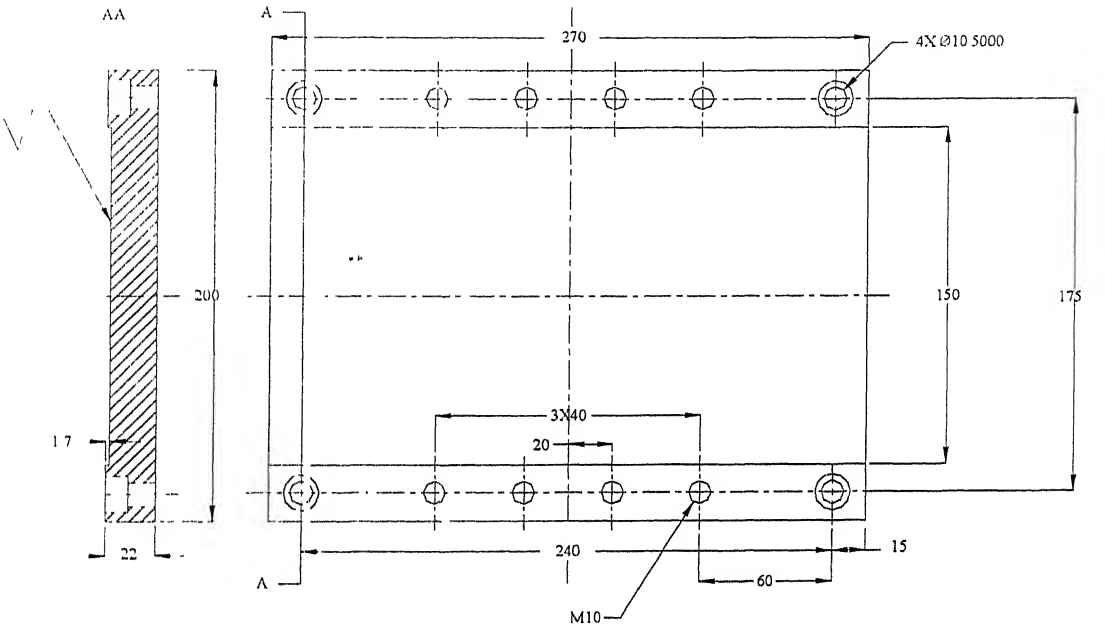

Fig. 2.8(a) Rear mount plate with a shallow groove to hold specimen

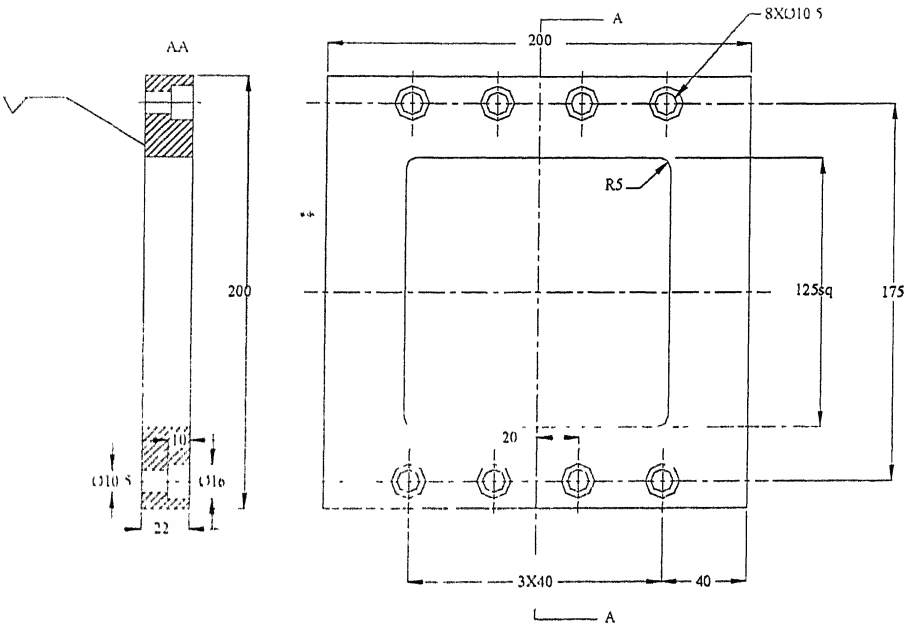

Fig. 2.8(b) Front mount plate for clamping the specimen

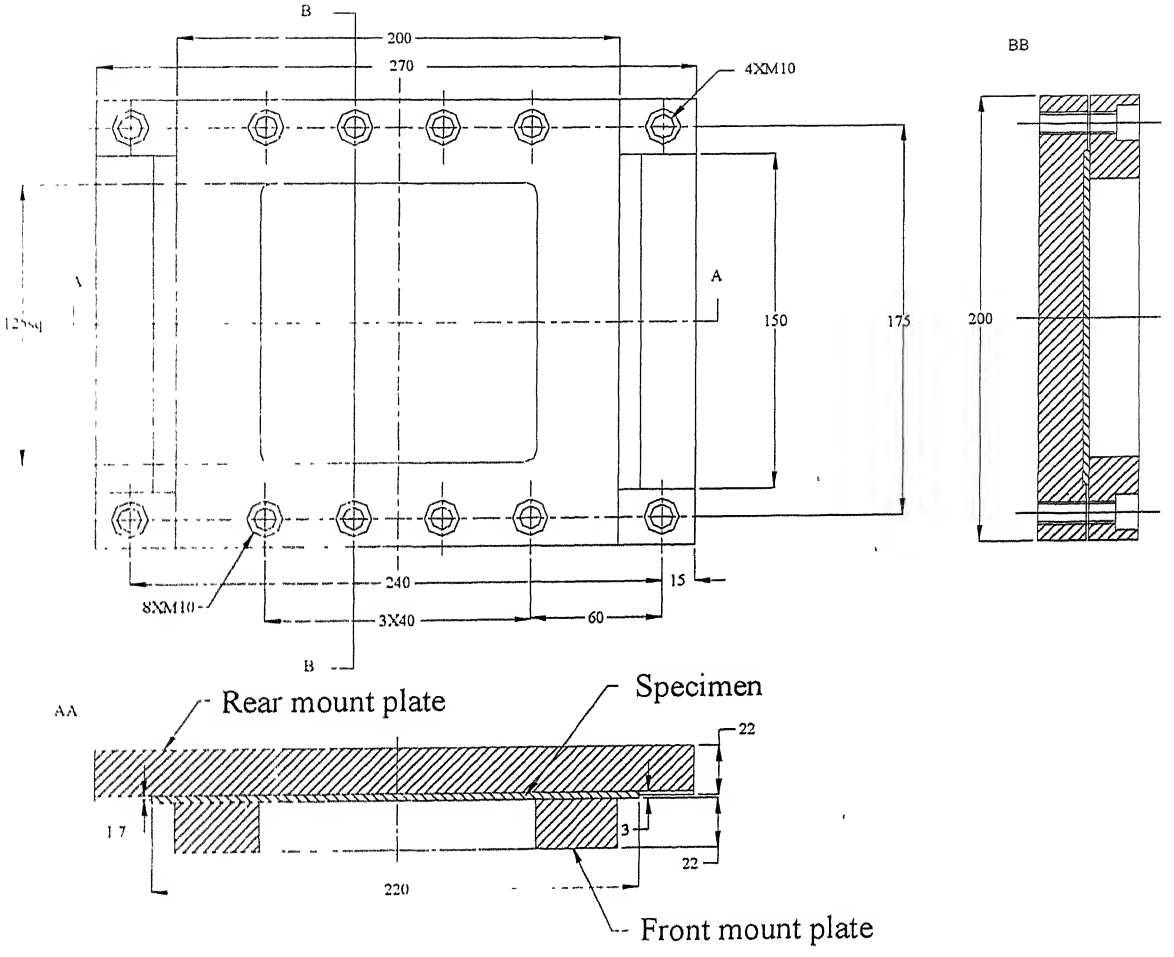

Fig. 2.9 Assembly of specimen with mounting plates

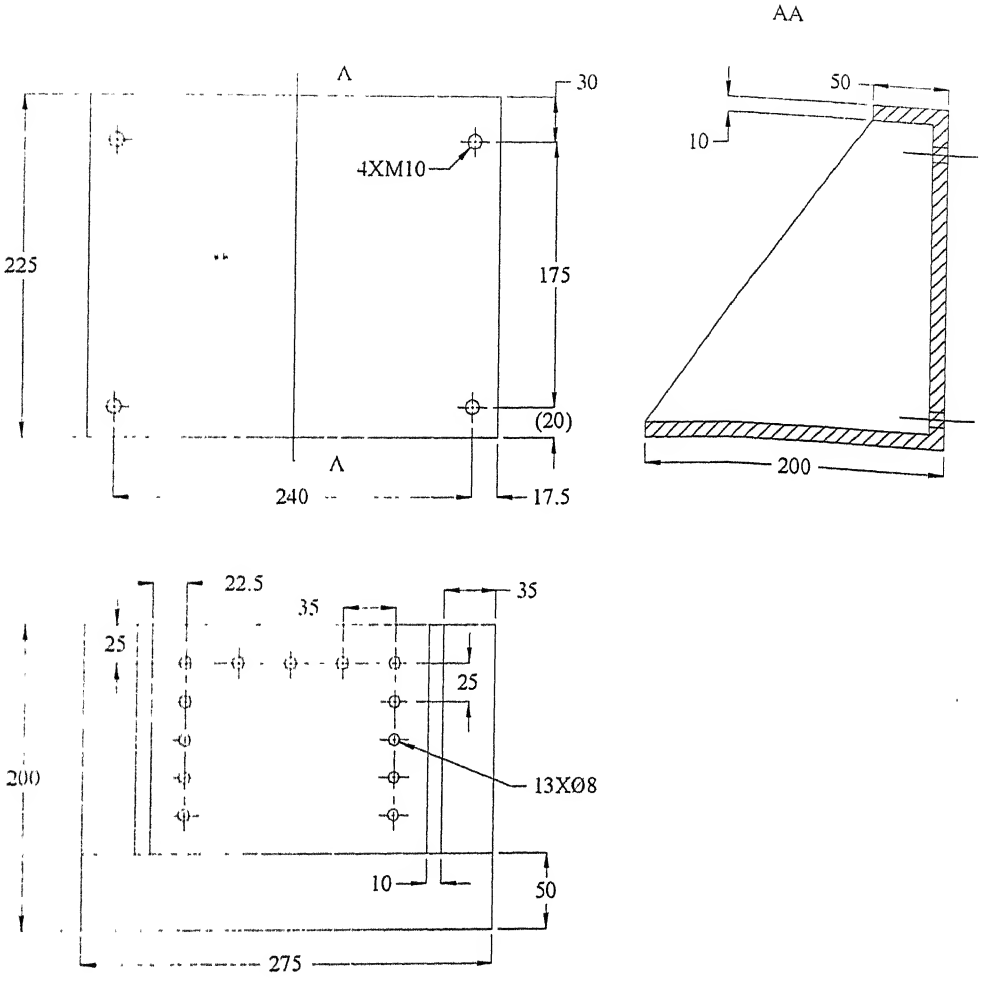

Fig. 2.10 Rear base frame for mounting the specimen assembly on bottom channel

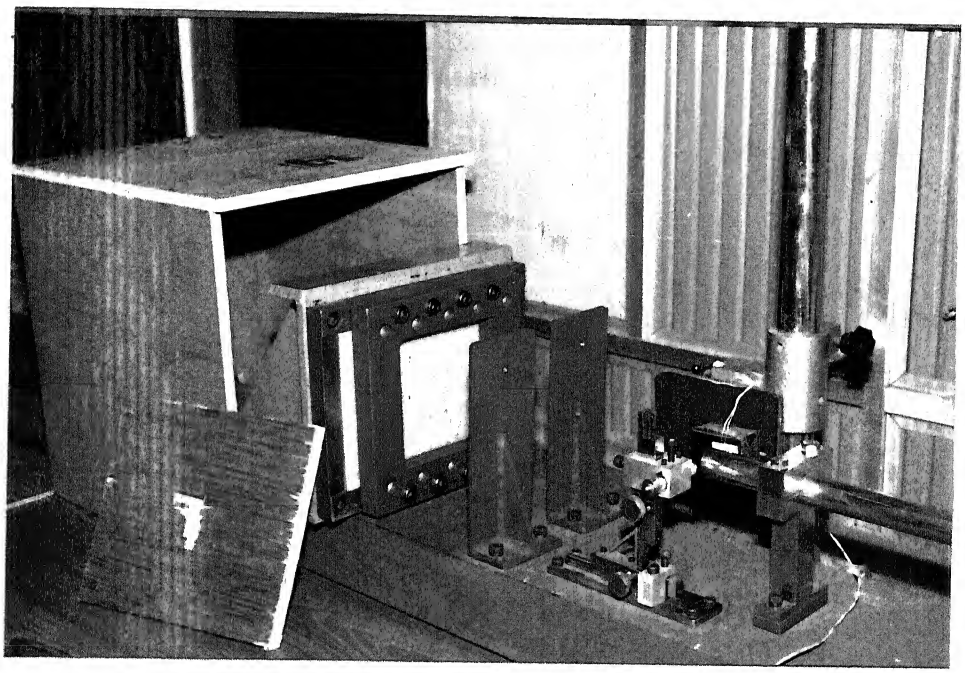

Fig. 2.11 A photograph showing specimen mount assembly mounted on the bottom channel

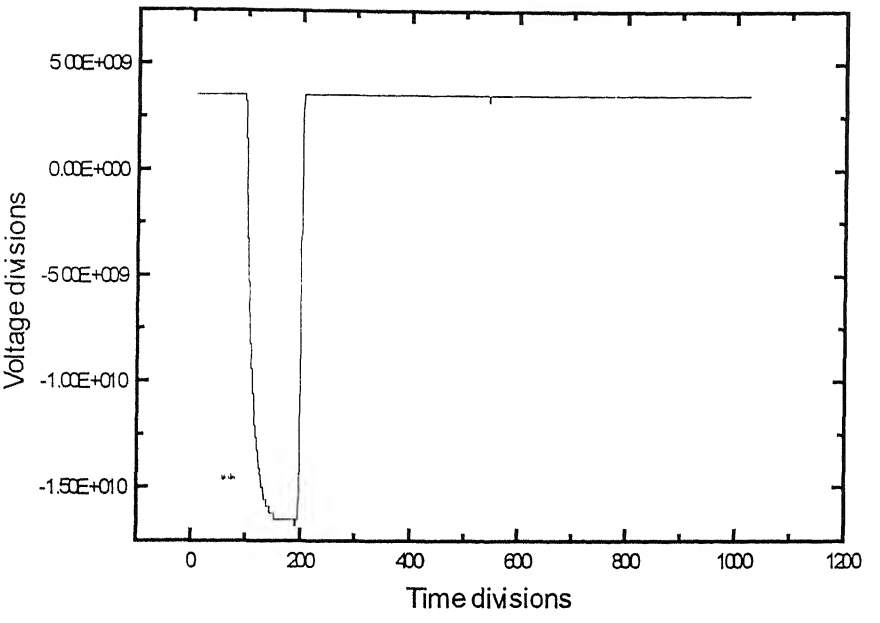

Fig. 2.12 The voltage pulse monitored by digital oscilloscope to determine projectile velocity

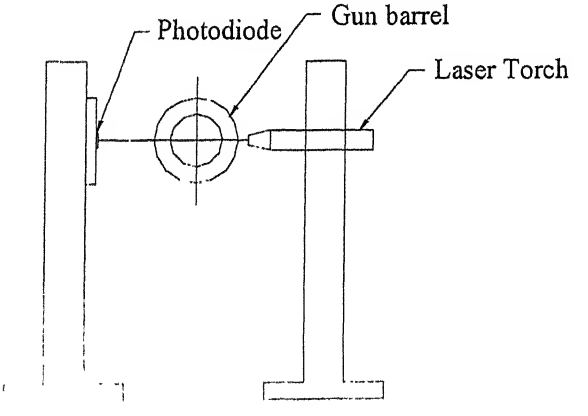

Fig. 2.13 Line diagram for velocity measurement

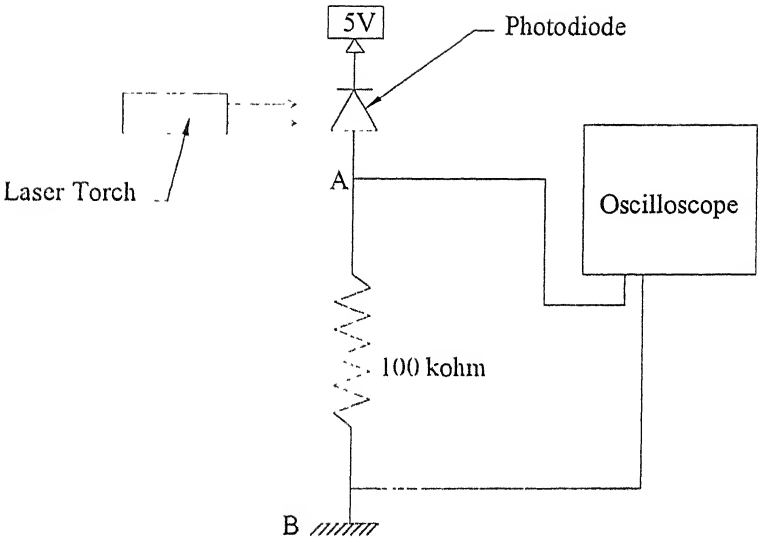

Fig. 2.15 Circuit diagram for velocity measurement of projectile

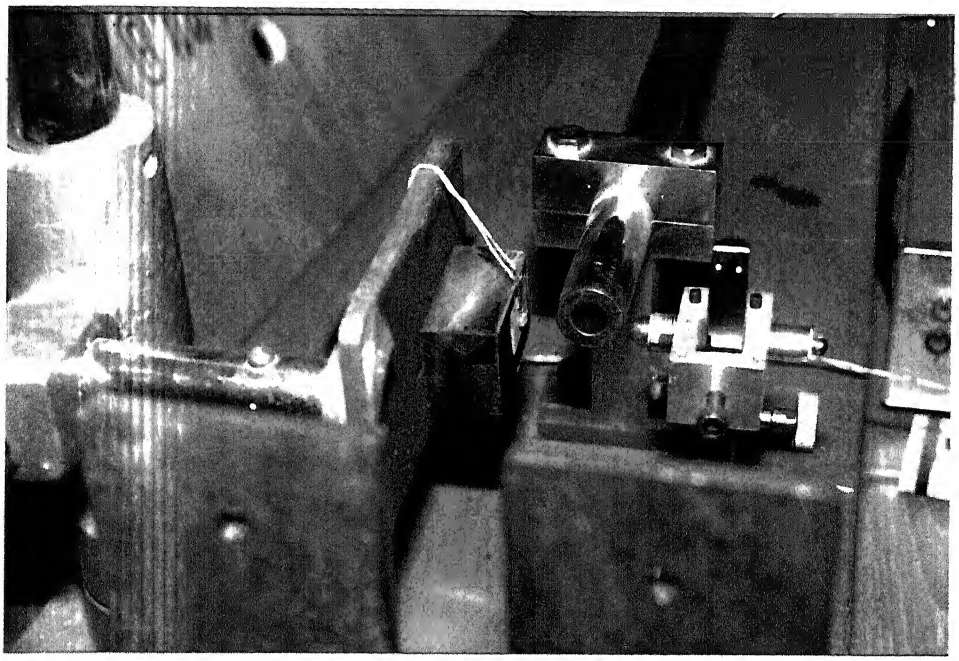

Fig. 2.14 A photograph showing the laser torch and photodiode inline with the gun barrel

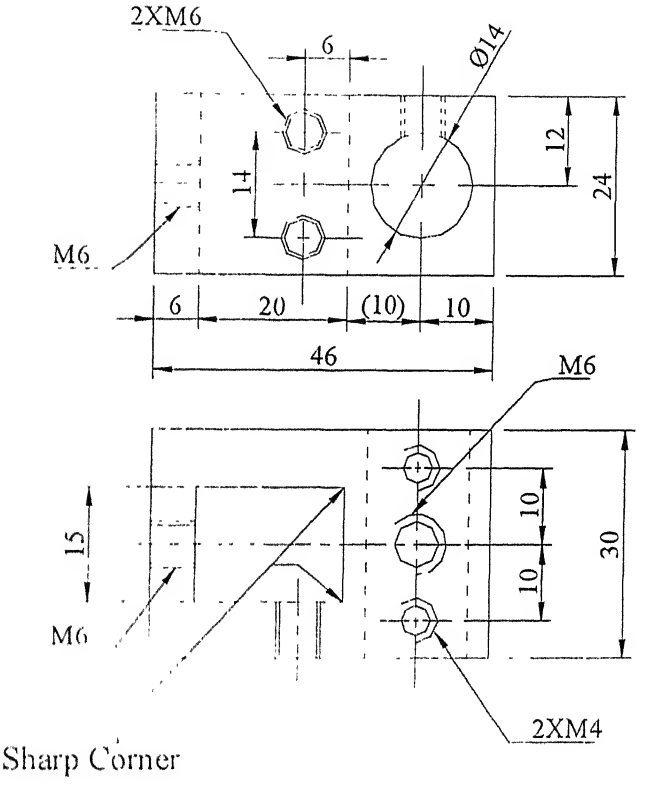

Fig. 2.16 Laser torch holding block

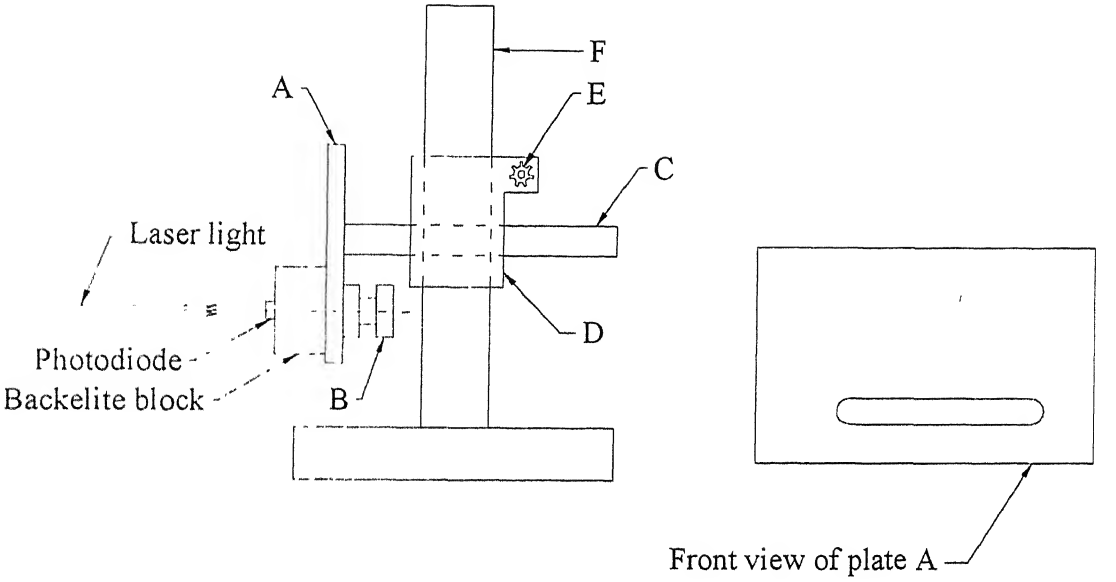

Fig. 2.17 Mounting stand for photodiode

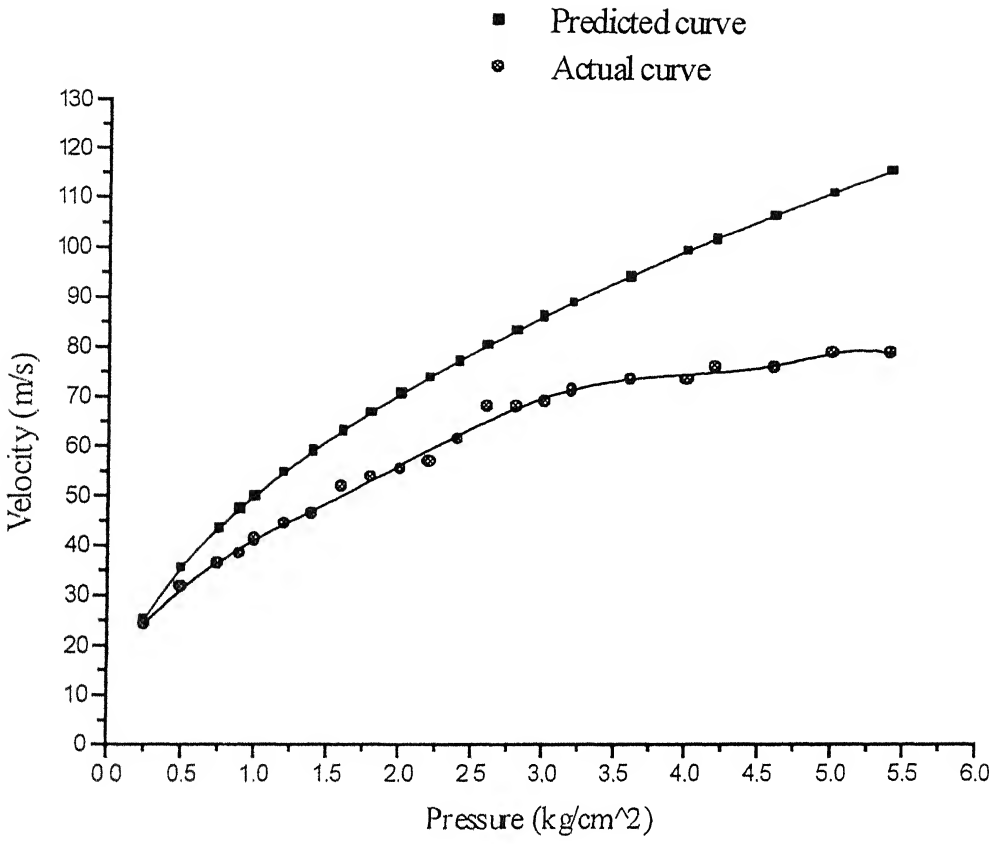

Fig. 2.18(a) Estimated and actual velocity of a steel projectile of 8.18 gm

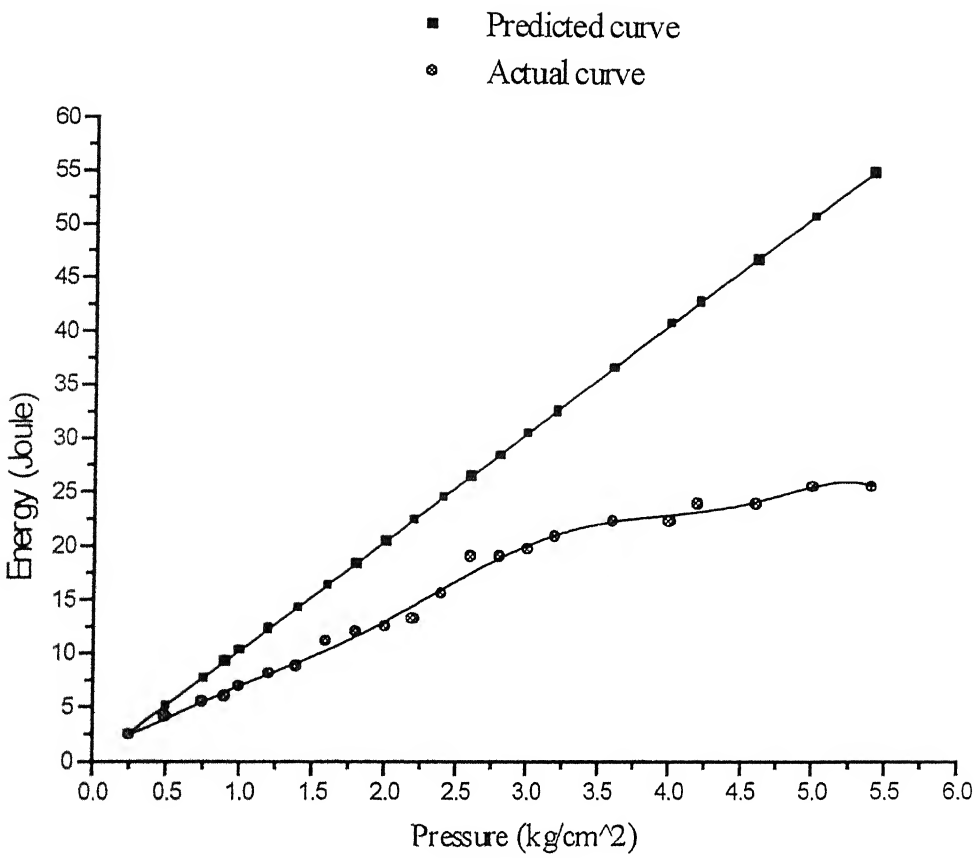

Fig. 2.18(b) Energy of a steel projectile of 8.18 gm

CHAPTER 3

COMPRESSION AFTER IMPACT TEST

3.1 INTRODUCTION

This chapter deals with the concept of Compression after Impact test. The procedure of impact test on a FRP panel by a foreign body has already been discussed in previous chapter. After the impact it is of interest to find the compressive strength of the damaged panel.

In the present chapter emphasis is given to the development of an experimental setup for evaluating the residual compressive strength of composite panels. The setup is designed to avoid buckling of the panel during testing.

3.2 SPECIMEN USED

Thin polymer composite impacted panels are employed for the compression test in this study. This section deals with the specimen geometry and preparation of specimen from impacted panels. The dimensions of the specimen used are as per shown in Fig. 3.1.

The preparation of panels for impact test is described in Chapter 2. The panels after impact test are trimmed from both the sides to have the width of 100 mm. To each end of a panel tabs of 60 mm length are bonded on both sides to have a test area of 100mm×100mm, as shown in Fig. 3.1. The impacted specimens ready for the compression test with two different thickness are shown in Figs. 3.2(a) and 3.2(b). Tabs are prepared from glass fabric reinforced polymer composite and are of 2 mm thickness. Its raw material and preparation is same as the specimen for impact. 16 plies of glass fabric prepreg are used for the preparation of tabs. Strain gauges are bonded on both the

faces (back-to-back) at 25 mm from the tab ends as well as from the sides of the specimen on point I as shown in Fig. 3.3. The outputs of both the strain gauges are monitored continuously during the experimentation to check whether buckling is initiated. Rectangles ABCD and A'B'C'D' are marked on the tabs to align the specimen in the grips of machine whereas rectangle EFGH is marked to assure the proper setting of buckling guides (explained in next Sec.).

3.3 COMPRESSION TEST

Static uniaxial compression test is done to evaluate the residual compressive strength of FRP panels after impact. Material Testing System (MTS) 810 machine is used for compression test. Machine has the load capacity of 100 kN. Machine uses a hydraulic power supply, which provides hydraulic fluid under pressure upto 21 MPa, to servovalves for actuator operation. Machine has Hydraulic wedge grip (model number 647) to clamp the specimen for testing purpose and a microconsole (model number 458.20) for its electronic control.

The biggest problem in the compression test is the geometric buckling specially in case of thin panels. This problem lead to the design of buckling guides made of mild steel, having 144mm×140mm outer dimensions. The buckling guide is made of two plates named front buckling guide and rear buckling guide as shown in Figs. 3.4(a) and 3.3(b). The guides are designed to be very stiff and strong. Each has an 80mm square hole in the center with a ridge of 5mm in width and 4 mm height all around the periphery of the square hole as shown. The top edge of the ridge is made flat and smooth through grinding. After the grinding, both edges of the ridge are made rounded so that only 2mm central portion of the flat remains plane. The guides are clamped around the specimen with four M12 bolts. The assembly of specimen with the buckling guides is shown in Fig. 3.5. The assembly is made by inserting rubber pads between the front and rear buckling guides. The rubber pads work as spring and make the guiding fixture as double acting; that is, untightening the screws increases the distance between the guides. The distance

between the two guides is adjusted to be only marginally higher than the specimen thickness (within 0.05 mm) with the help of feeler gauges.

The buckling guide assembly is heavy because they are made of thick mild steel plates. The dead weight of these guides should not be supported on the specimen. Chamfered edge holes are made in both the buckling guides such that the holes are in line and a strong but flexible string is passed through the holes and tied to the top frame of the MTS machine. Two such strings, one on each side, support the weight of the buckling guide.

Two types of data are recorded during the test, applied load and strains in the direction of load. The applied load is measured by means of a load cell that is provided with the testing machine. The strain in the direction of loading are measured by using the electrical foil type strain gauges. The testing-machine head movement is not a reliable measure of strain because some error may result from the compression of the specimen ends. The strain gauges are mounted on the specimen as shown in Fig. 3.1 and monitored during the test. Strain gauges with resistance of 120 ± 0.2 Ω and a gauge length of 2 mm having gauge factor of 2.11 are used. Strain gauges are imported from Tokyo Sokki Kenkyujo Co. Ltd., Tokyo, Japan and specially designed to be used for composite materials. Load cell and strain gauges are connected to the virtual instrumentation (VI) to monitor them continuously during the test. Details on VI are discussed in the subsequent sections.

3.4 VIRTUAL INSTRUMENTATION

Virtual instrumentation is used in the present work for measuring strains and load simultaneously. Fig. 3.6 shows the block diagram of the virtual instrumentation set up. The signals from the strain gauges are fed to a strain gauge signal condition card (model SC 2403-SG, National Instruments, USA). The strain gauge signal condition card is configured for recording signals in quarter bridge mode. The signals are then fed to an analog to digital card (model PCI 6024E, National Instruments, USA) for conversion of

analog signals to digital signals. A virtual instrument is developed using LABVIEW program for recording the signals from strain gauges and load signal from the load cell.

The virtual instrument, front panel and wiring diagram are shown in Fig. 3.7 and Fig. 3.8. This virtual instrument is designed for data logging of eight strain gauge inputs and one load input from the load cell. Presently, only two strains input and one load input is used. In wiring diagram a provision is made to convert the input strain gauge voltage into direct strain using the formula node. Another provision is also made to record strain and load readings on the hard disk of the computer in ASCII format as a text file As this file is compatible to spreadsheet format, e.g., Microsoft excel, Grapher, MicroCal origin etc., the analysis of data can be done by importing the file into the particular software.

3.5 EXPERIMENTAL PROCEDURE

The experimental procedure starts with checking of the entire MTS tensile machine through a dummy steel specimen (shown in Fig. 3.2(a)) having thickness of 10 mm and lateral dimensions of 220mm×100mm. The steel specimen is ground flat on both the side and strain gauges are placed at the center on both the faces (back-to-back) to check the proper working of machine. The result (Fig. 3.9) shows the proper working of machine and V I (virtual instrument) software. A loaded FRP specimen in machine is shown in Fig. 3.10(a). The specimen is mounted in the machine, using the wedge section friction grips of machine, upto the depth of 30 mm from both the ends. The proper alignment of the specimen in the jaws is assured by aligning the specimen in the jaws using rectangles ABCD and A'B'C'D' as shown in Fig. 3.2. The proper spacing between the two buckling guide plates and specimen is set within 0.02 mm using BOPP feeler gauges. Buckling guides are hanged symmetrically on to the top frame of machine as described previously in the Chapter. The strain gauges and load cell are then connected to the VI as described earlier. Fig. 3.10(b) shows the V I arrangement used for strain measurement.

After mounting the specimen on to the machine it is loaded monotonically upto the failure at a rate of 4.0 mm/min. The data (load and strains) are continuously recorded in the computer during the test through the VI. Load v/s strain curves are plotted using these data. One typical result is shown in Fig. 3.11. The test was conducted on a glass fabric reinforced FRP panel of the dimensions as shown in Fig. 3.1. The results show that the strains are almost same upto certain amount of compressive load and then start diverging. The divergence point is taken to be the compressive strength.

3.5 CLOUSRE

The work presented in this chapter consists of the development of CAI test setup. Design of a buckling guide arrangement is presented. A virtual instrument is developed for measuring the strains and applied load. The front and wiring diagram of virtual instrumentation are also shown in this chapter.

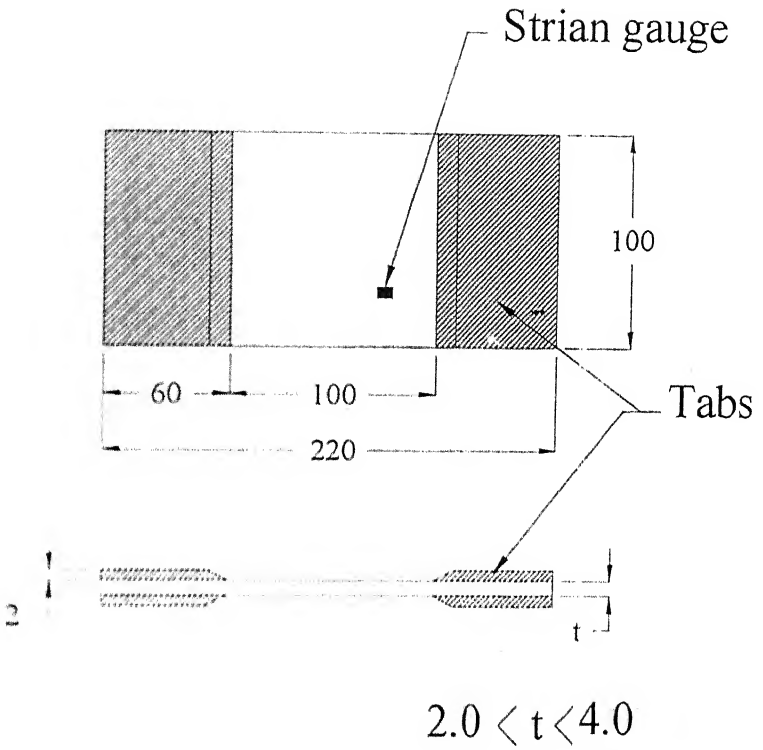

Fig. 3.1 Specimen used for Compression after impact test

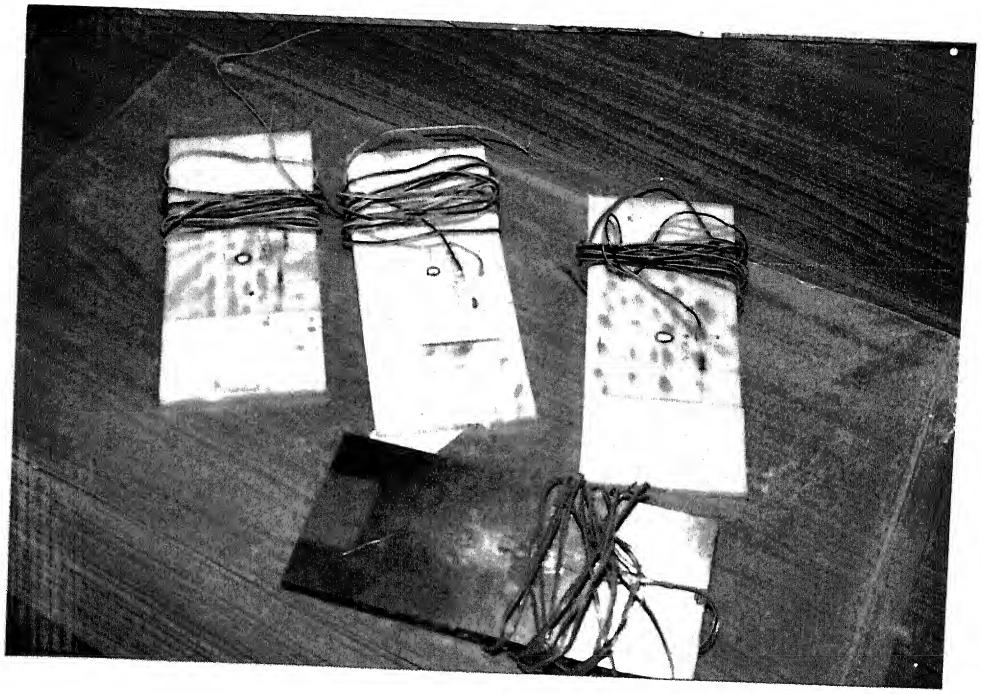

Fig. 3.2(a) Thin impacted specimens ready for compression test (including the steel specimen to check the MTS machine)

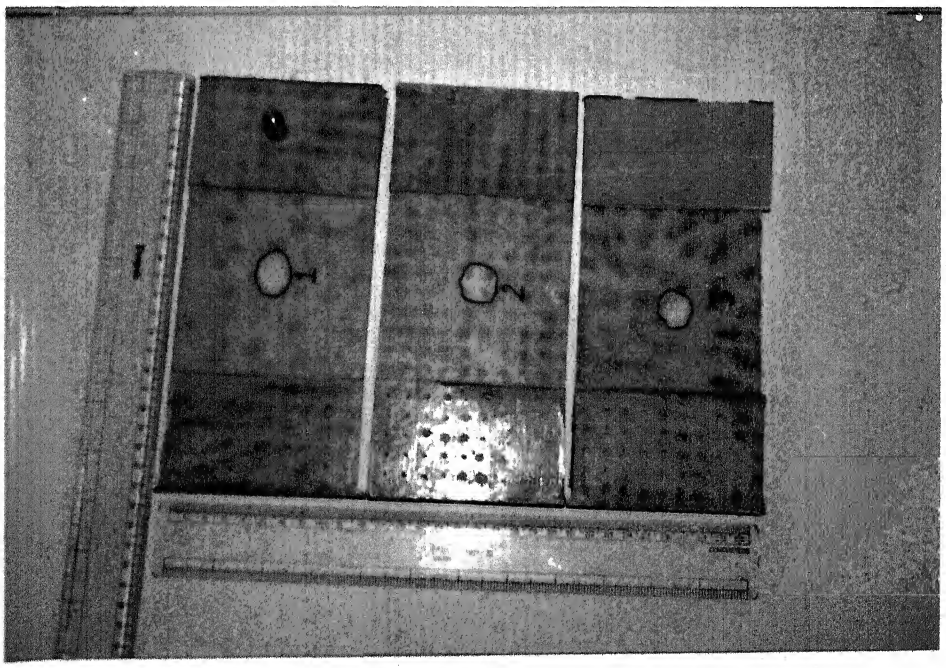

Fig 3.2(b) Thick impacted specimens ready for compression test

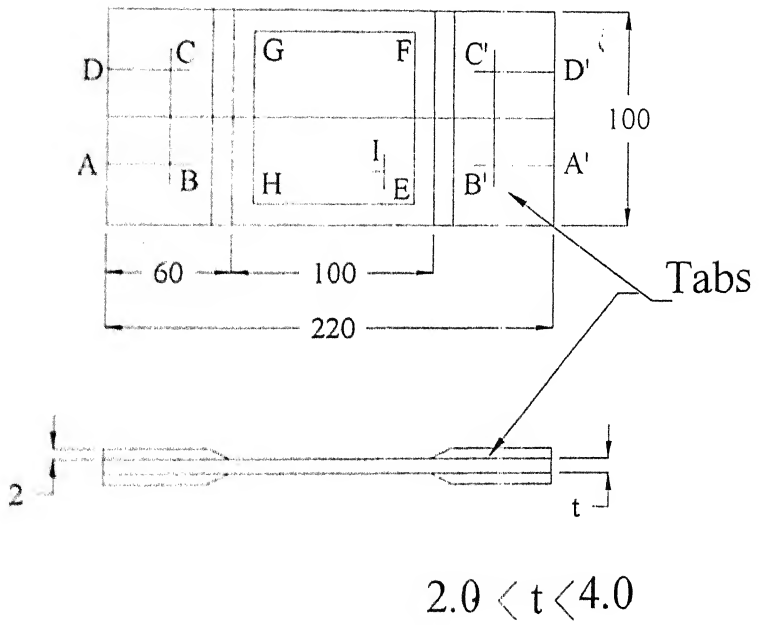

Fig. 3.3 Marked Specimen before mounting the strain gauge over it

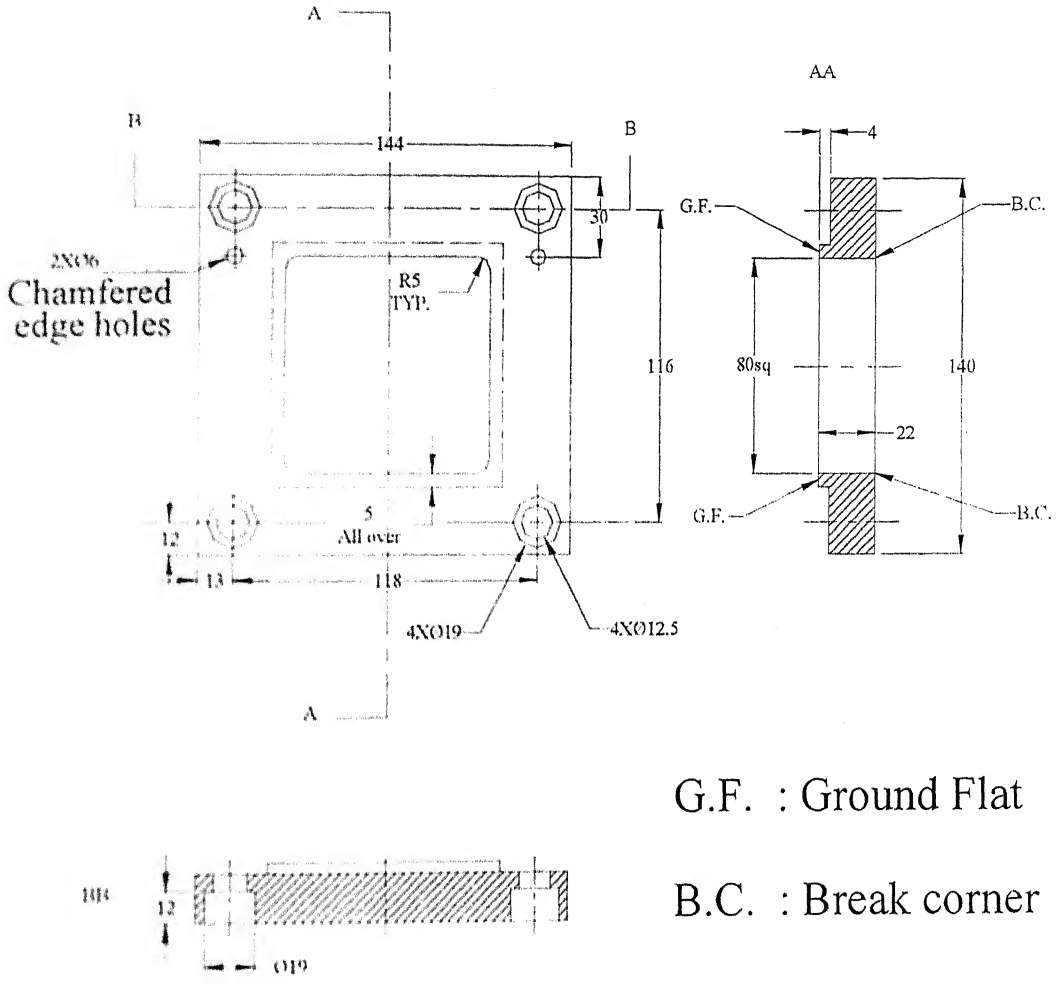

Fig. 3.4(a) Front Buckling Guide plate

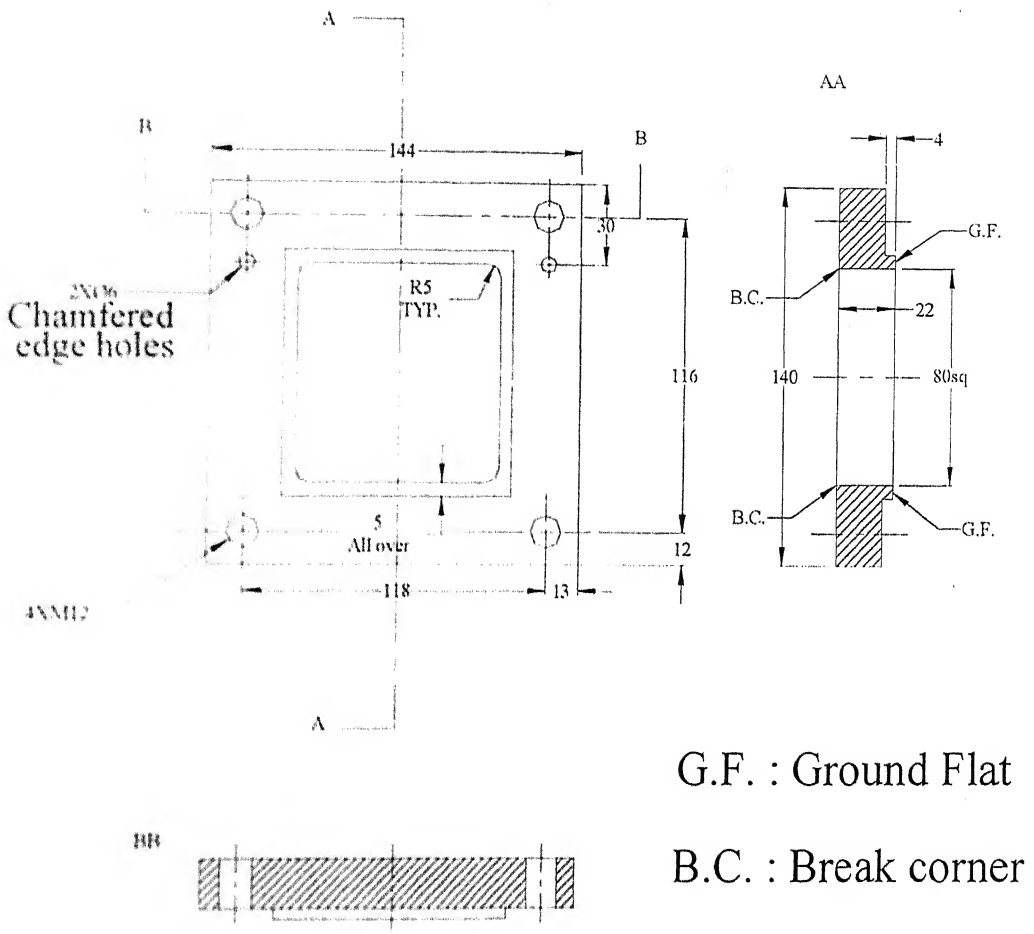

Fig. 3.4(b) Rear Buckling Guide Plate

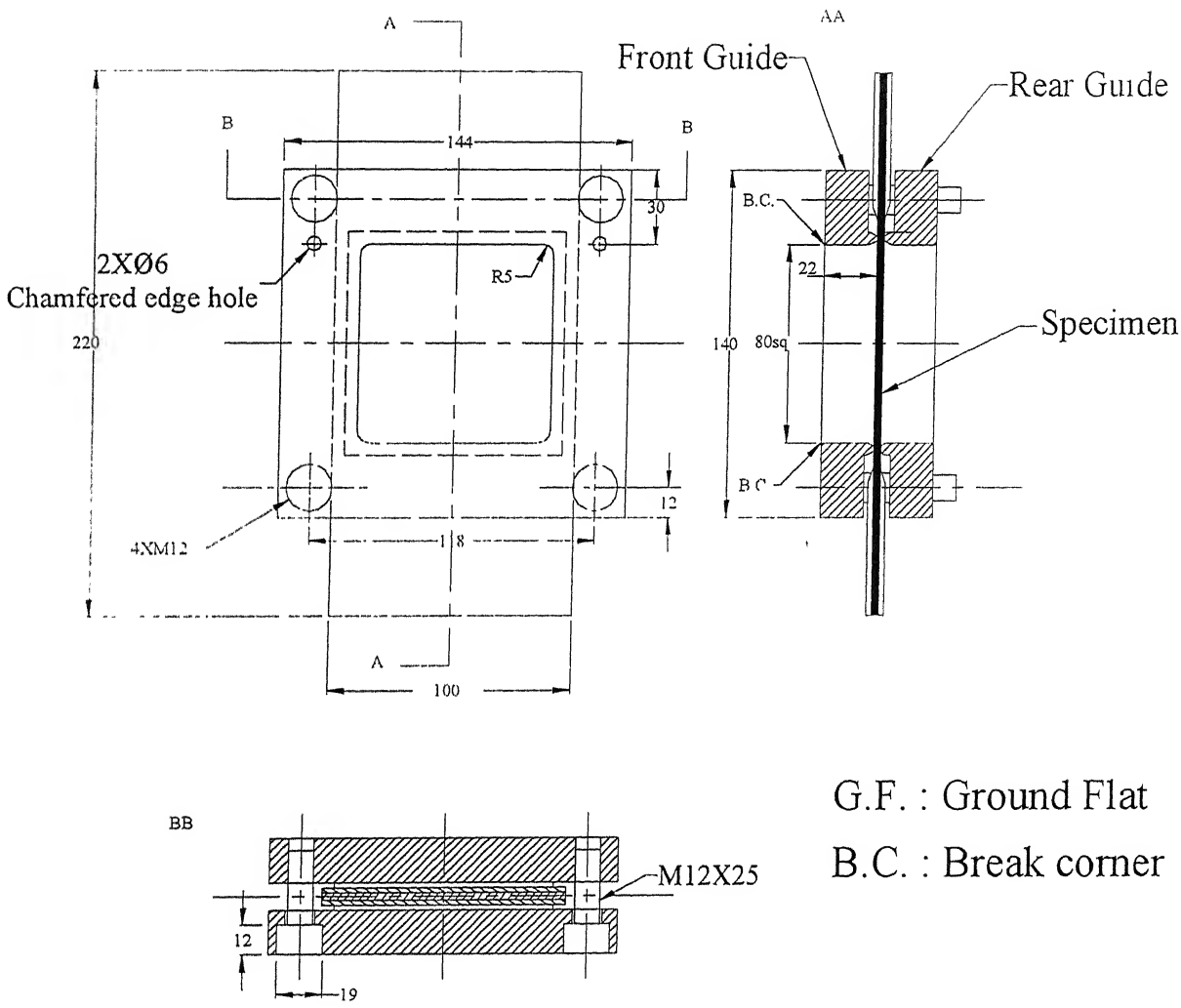

Fig. 3.5 Assembly of Specimen with buckling guides

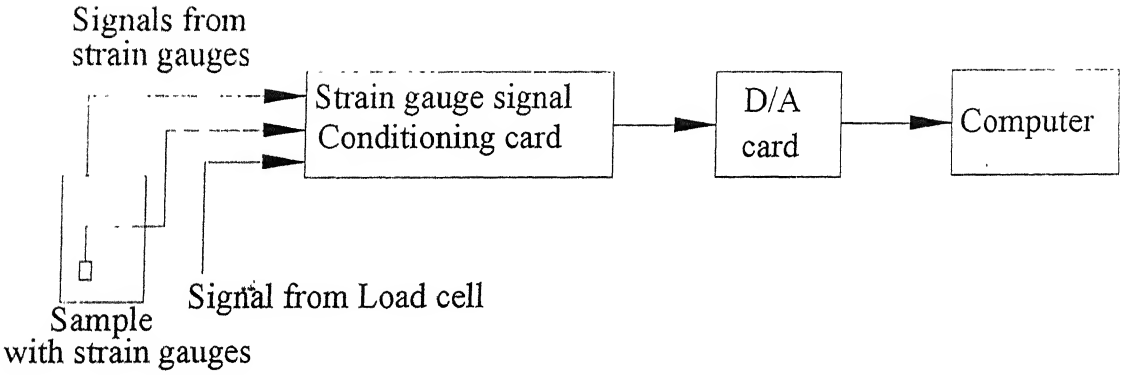

Fig. 3.6 Schematic diagram of the Virtual Instrumentation Setup using a D/A Card

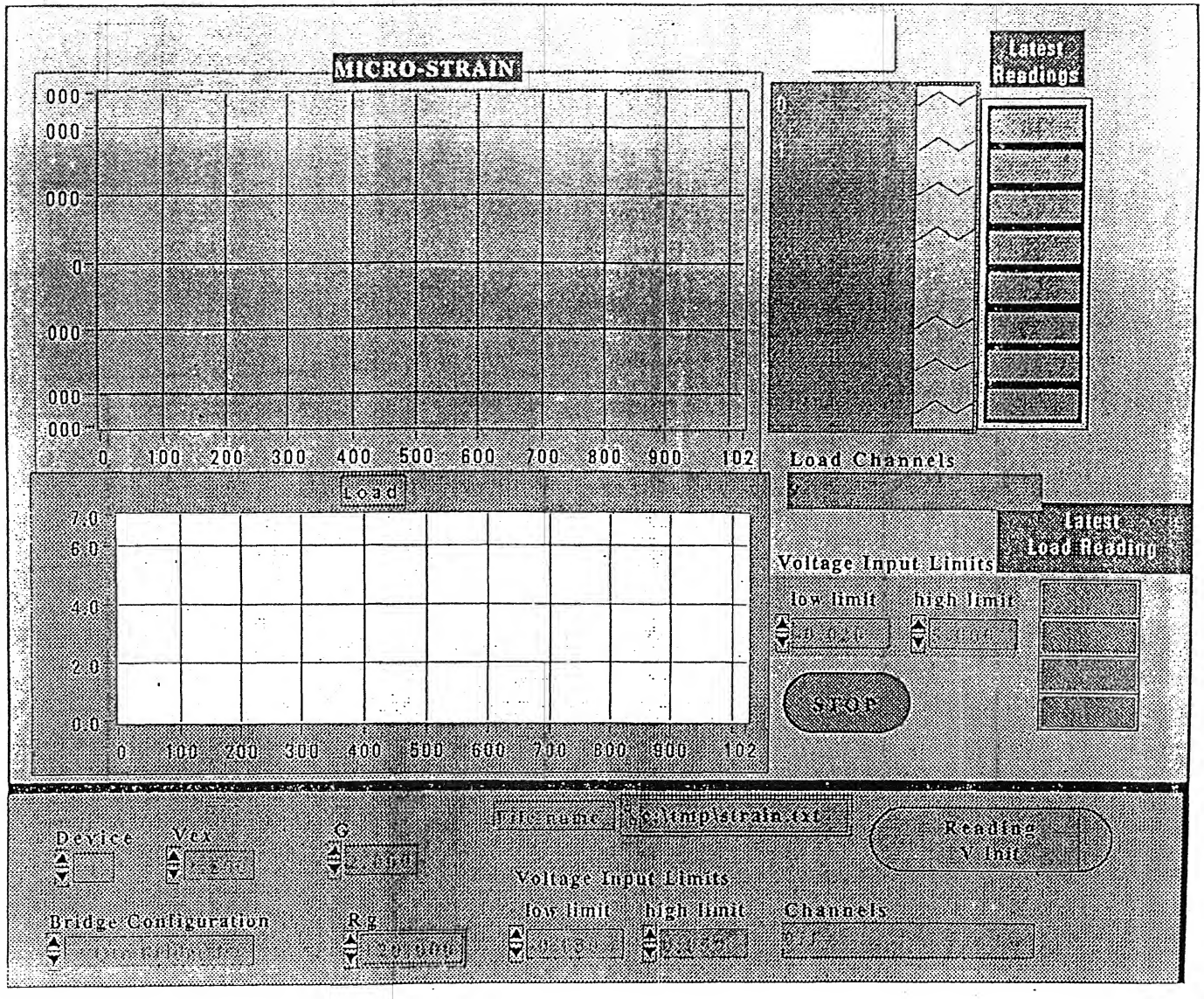

Fig 3.7 Front panel of Virtual Instrumentation (LABVIEW)

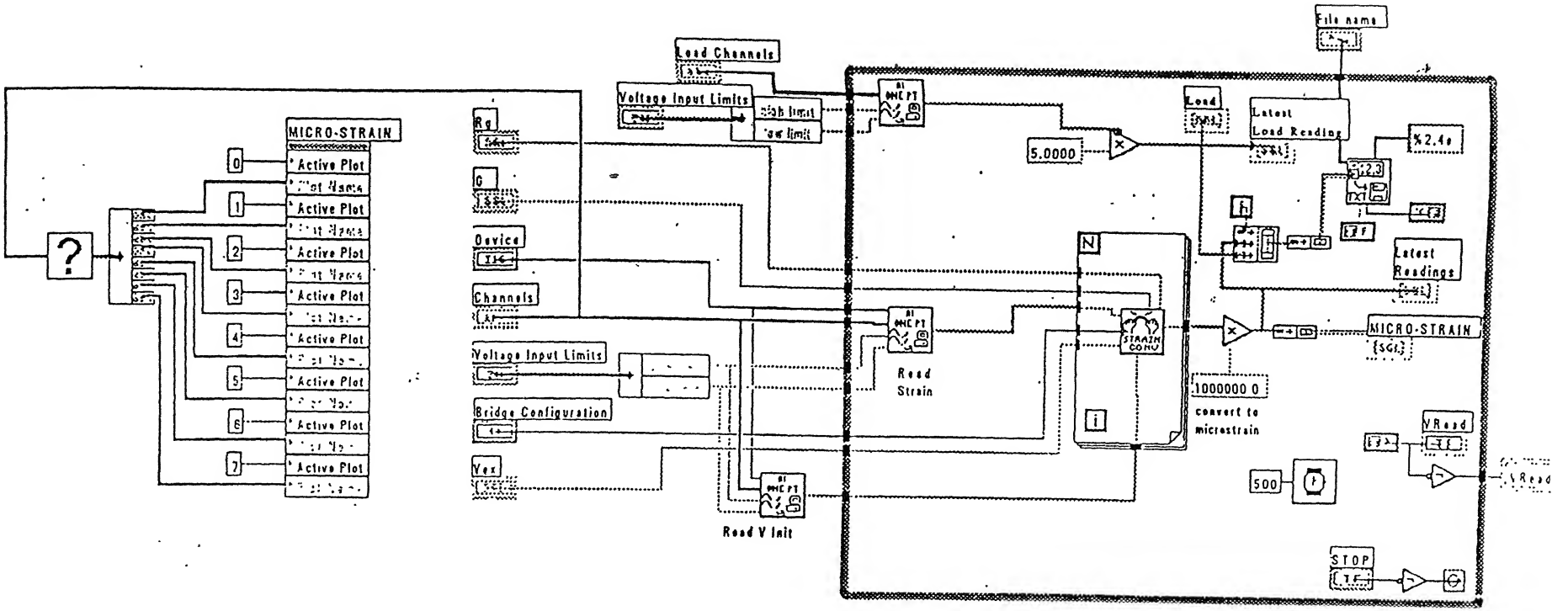

Fig. 3.8 Wiring diagram for Virtual Instrumentation (LABVIEW)

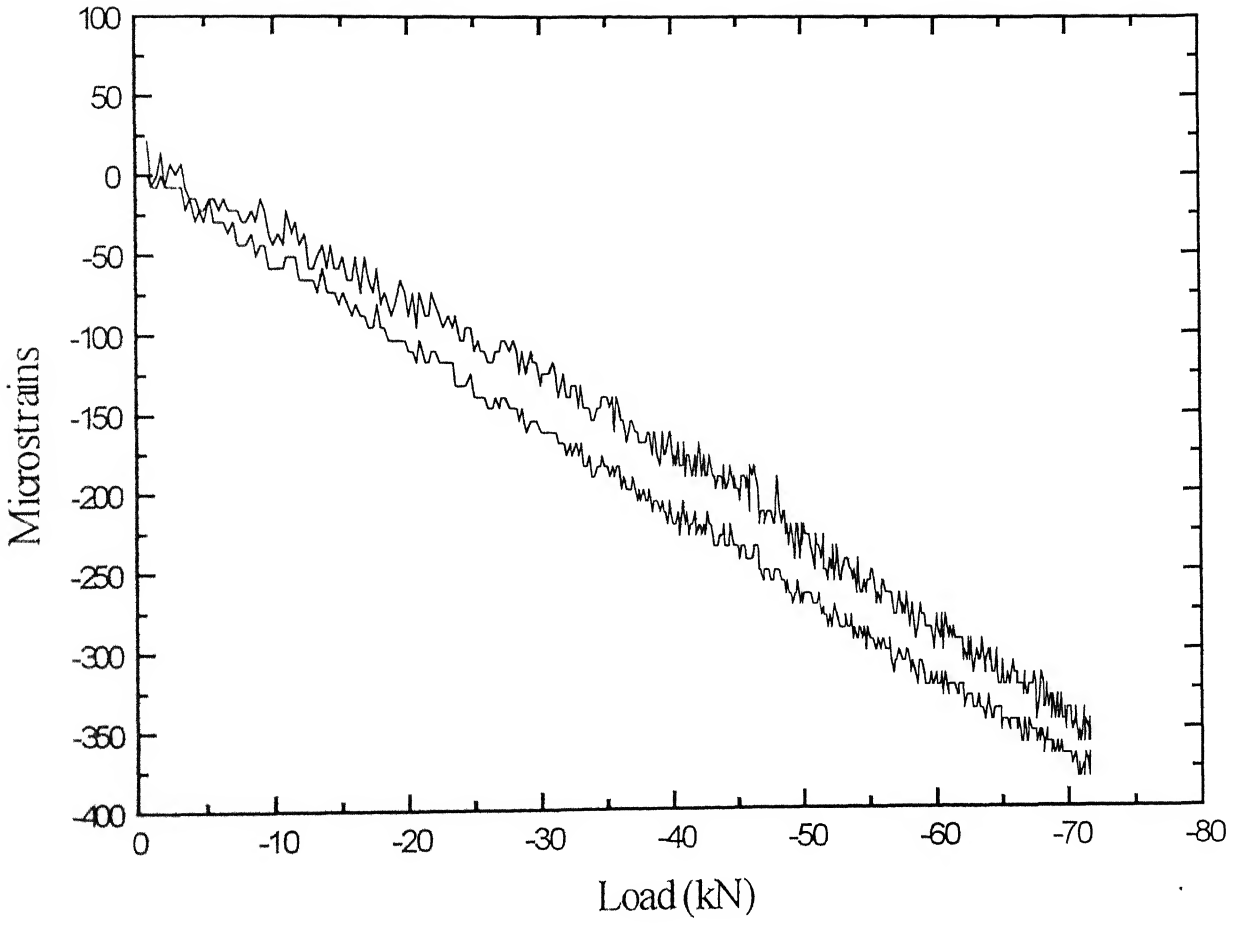

Fig. 3.9 Microstrains in steel specimen during checking the machine

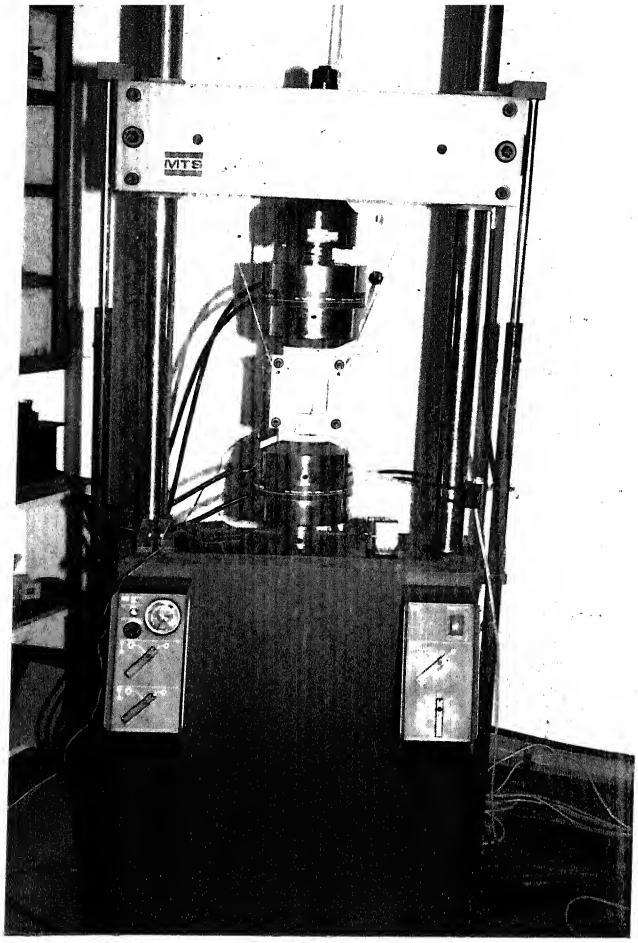

Fig. 3.10(a) A FRP specimen loaded in MTS tensile machine with buckling guide

Fig. 3.10(b) Virtual instrumentation arrangement for strain measurement

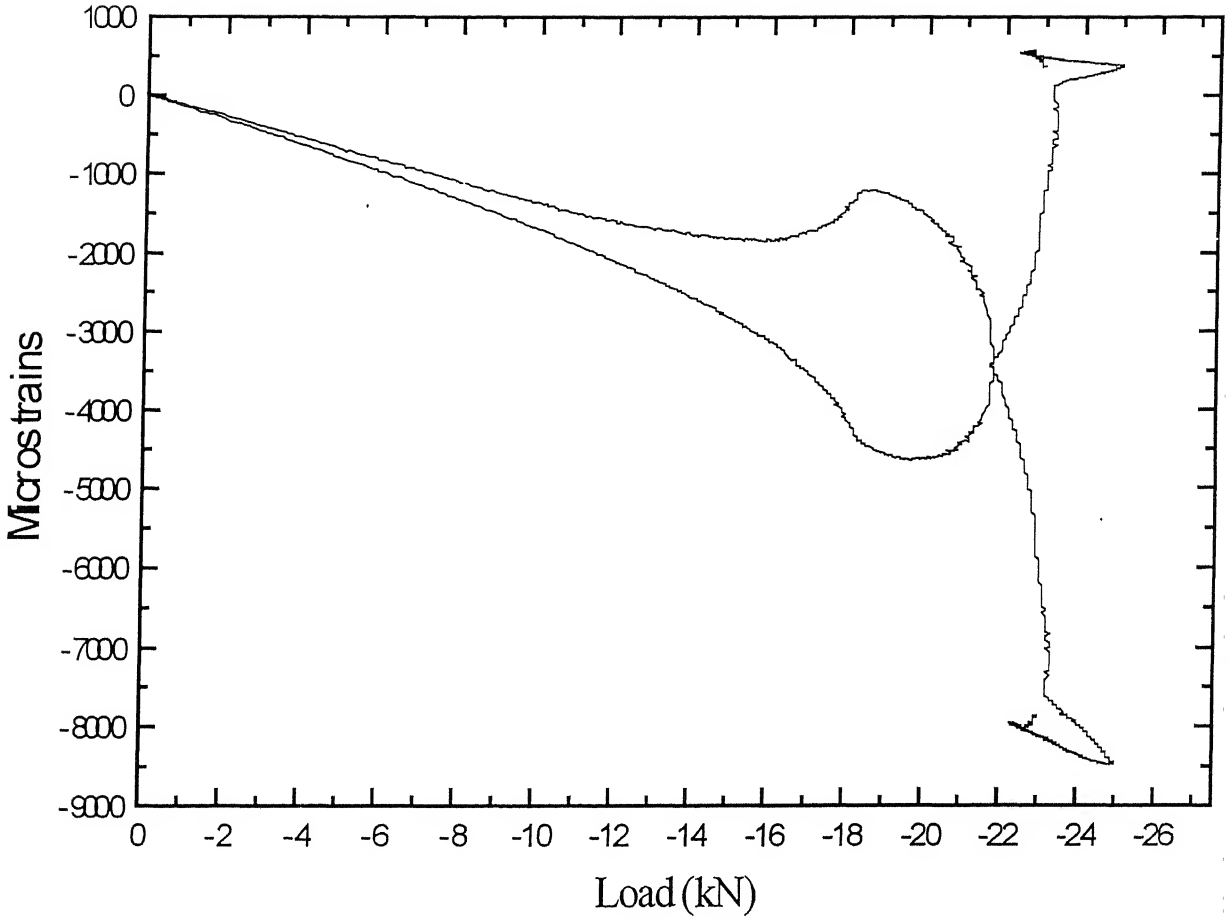

Fig. 3.11 Microstrains in thin composite panels against the Load

CHAPTER 4

RESULTS AND DISCUSSION

4.1 INTRODUCTION

This chapter deals with the results obtained from the tests performed on the FRP panels with the test setup described in Chapter 2 and Chapter 3. The specimens are prepared from glass fabric/epoxy. The specimens are first impacted using air gun impact test setup. The impacted specimens are then taken to the compression test (CAI test).

Two kinds of specimen are used to perform the impact and compression tests, thin and thick specimens. Thin specimens have their thickness ranging from 2.5 to 3.0 mm whereas thicker specimens have their thickness above 3.5 mm.

4.2 THIN SPECIMEN

Thin specimens have thickness less than 3.0 mm. Specimen details with impact level and damage area are given in Table 4.1.

Table 4.1 Details of thin specimen

S.No.	Specimen No.	Thickness (mm)	Impact level (Joule)	Damage area (cm^2)
1.	A1	2.54	6.15	0.45
2.	A2	2.70	6.15	0.50
3.	A3	2.60	6.38	0.50

The impacted specimens have been tested for their compressive strength after impact. Load verses Strain curves obtained during the compression test are shown in Figs. 4.1, 4.2 and 4.3 corresponding to the specimens A1, A2 and A3 respectively. Each specimen fails in buckling at points A and B as shown in the corresponding figure.

The flexural rigidity EI, where E is the modulus and I moment of inertia, of thin panels is on low side. This is because the modulus of glass fiber fabric composites is of the order of 26 GPa, substantially smaller than aluminium or steel, and the moment of inertia is proportional to the cube of the thickness. Consequently, thin panels under compressive load buckle easily. For example, in specimen A1, significant buckling is observed at 14 kN load (Fig. 4.1), which corresponds to only 55 MPa compressive stress. On further increase of load, the panel buckles excessively; so much so, that strain gauge on outer side starts showing tensile strain. In fact a stage reaches, when panel's ability of taking compressive load starts decreasing. Furthermore, in this panel with a small damage area (0.45 cm^2), no growth of damage area was observed throughout the loading cycle.

The response of specimen A2 is similar to that of specimen A1. Significant buckling is observed at compressive load of 10 kN corresponding to 37 MPa compressive stress. No growth of damage area was observed during loading. Specimen A3 shows the similar response with no growth of damage area.

Based on the results of thin specimens, it was realized that the geometric parameters of the specimen and impact loading parameters were not chosen properly. The flexural rigidity of the panel should be higher so that larger compressive stress can be applied. Also, the impact energy should be chosen properly so as to have larger impact damage area. Panels with large impact area are likely to fail under compressive load through the growth of the damage area.

4.3 THICK SPECIMEN

Thicker specimens have their thickness more than 3.5 mm. The specimen details with impact level and damage area are given in Table 4.2.

Table 4.1 Details of thick specimen

S.No.	Specimen No.	Thickness (mm)	Impact level (Joule)	Damage area (cm^2)
1.	B1	3.6	6.15	3.0
2.	B2	3.8	6.15	3.4

The impacted specimens have been tested for their compressive strength after impact. Load verses Strain curves obtained during the compression test are shown in Figs. 4.4 and 4.5 corresponding to the specimens A1 and A2 respectively. Each specimen fails due to delamination at points A and B as shown in the corresponding figure.

The material of thick specimen is same as that of thin specimen and therefore modulus remains same. However, thick specimen B1 is substantially thicker than specimen A1 with 2.85 times higher moment of inertia. Thus the flexural rigidity of thick panels is substantially larger. Although the impact energy level applied to specimen B1 is same as that of specimen A1 but the damage area of specimen B1 is substantially larger (6.7 times larger). The results show that the thick specimens are more susceptible to impact damage. Similar to specimen A1 the specimen B1 also start buckles at a compressive load of 14 kN (Fig. 4.4), which corresponds to 39 MPa compressive stress. This is probably due to larger damage in impact. But the failure mechanism of the thick specimen is quite different. Unlike specimen A1, specimen B1 does not buckle excessively at higher loads. The damage area started growing at about 16 kN (compressive stress of 44 MPa). When the compressive load approached to 22 kN (Fig. 4.4), which corresponds to 61 MPa compressive stress, the specimen failed; the damage

area grew through the width of specimen to both the free edges. Fig. 4.6 shows the failed specimen.

The response of specimen B2 is somewhat unexpected. Due to higher thickness the flexural rigidity of specimen B2 is 1.18 times higher than the flexural rigidity of specimen B1. The observed damage area of specimen B2 is 3.4 cm^2, which is 13% larger than that of specimen B1. The load-strain plot (Fig. 4.5) shows that buckling initiated at much higher compressive load of 30 kN, which corresponds to 79 MPa compressive stress. Unexpectedly, the damage area did not grow at all at high compressive loads. Instead, a damage initiated about 26 mm above the center of impact at about 32 kN load (compressive stress of 84 MPa). This initiated damage area grew sideways similar to the growth in specimen B1 all the way to both the edges. The final failure occurred at 45 kN load (compressive stress of 118 MPa). Fig. 4.7 shows the failed specimen.

Further experimentation is required to optimize to the geometric, material and impact parameters to have compressive failure through the growth of impact damage zone.

4.4 CLOSURE

The damage area is less in thin specimens rather than the thick specimens, which shows that the thick specimens were susceptible to large damage area in impact. Thin specimen failed through buckling only with no growth of damage area. Thick specimen failure due to growth of damage area was observed.

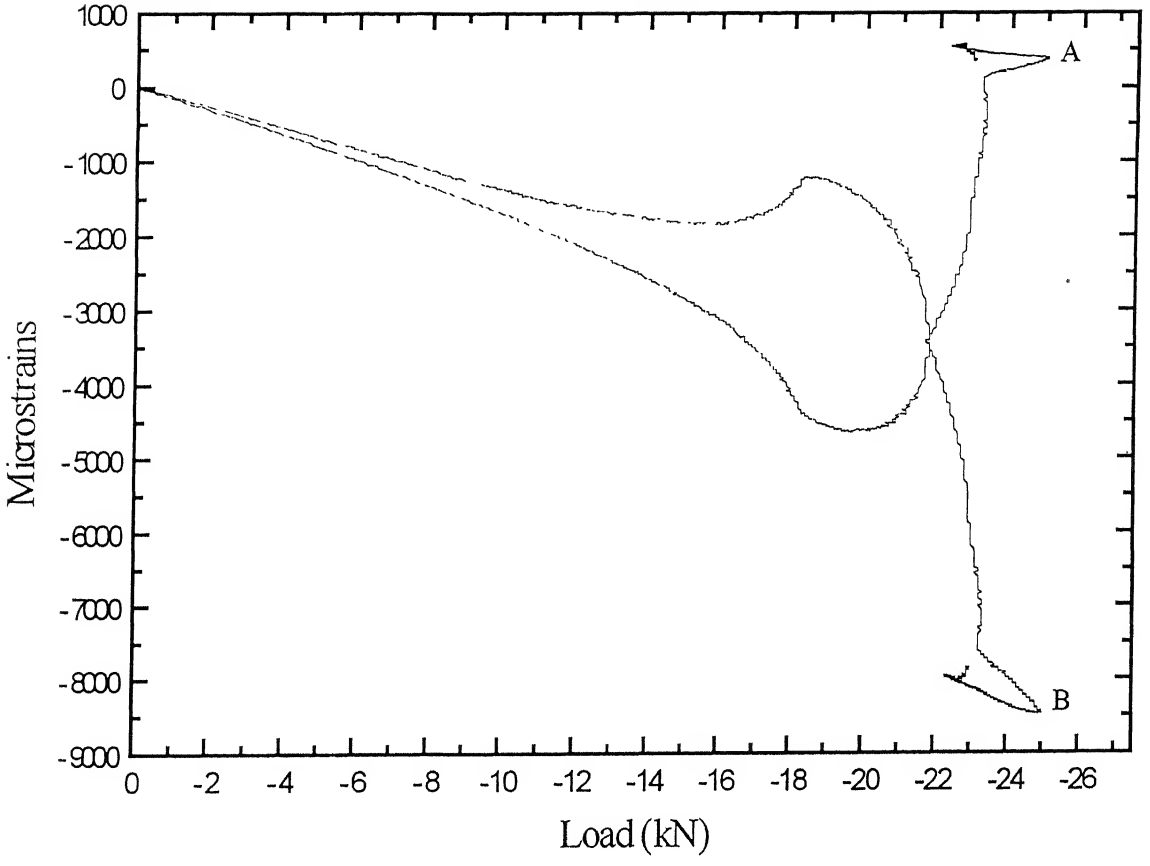

Fig. 4.1 Load verses strain curve for specimen A1

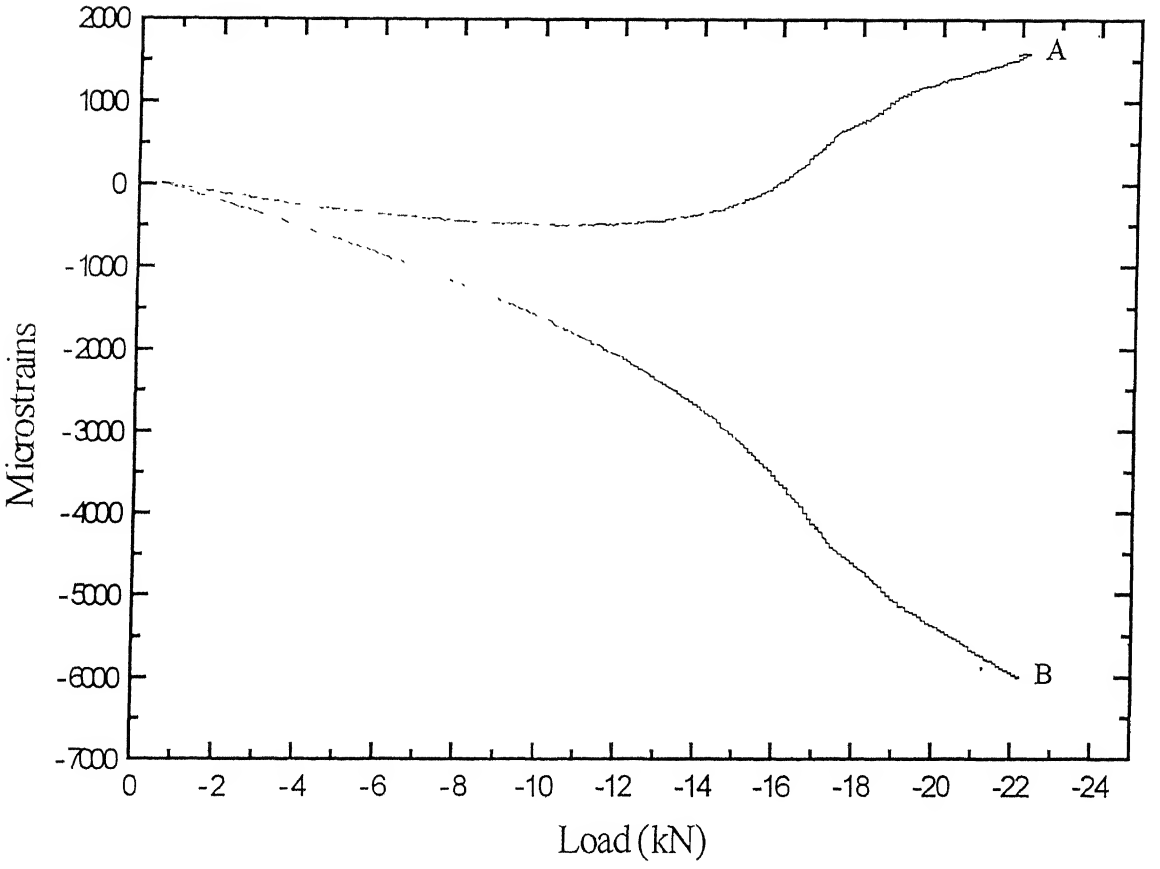

Fig. 4.2 Load verses strain plot for specimen A2

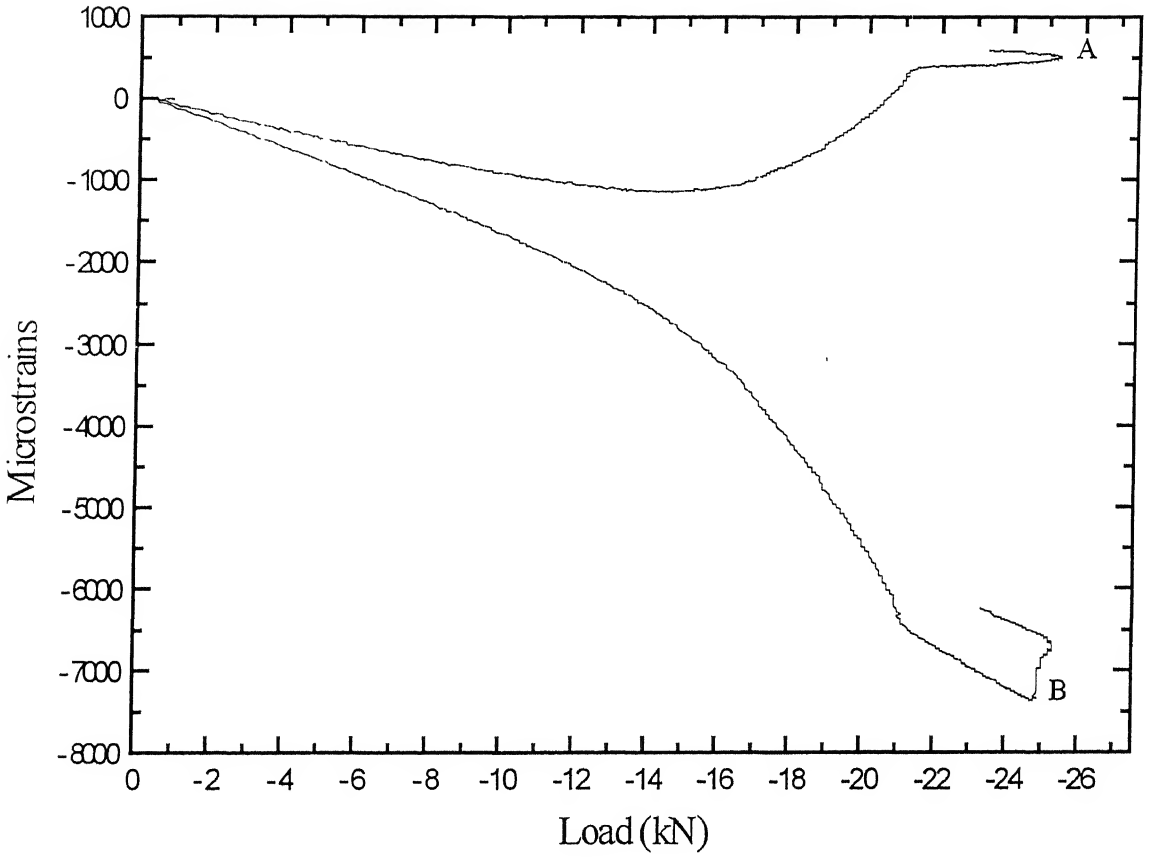

Fig. 4.3 Load verses strain curve for specimen A3

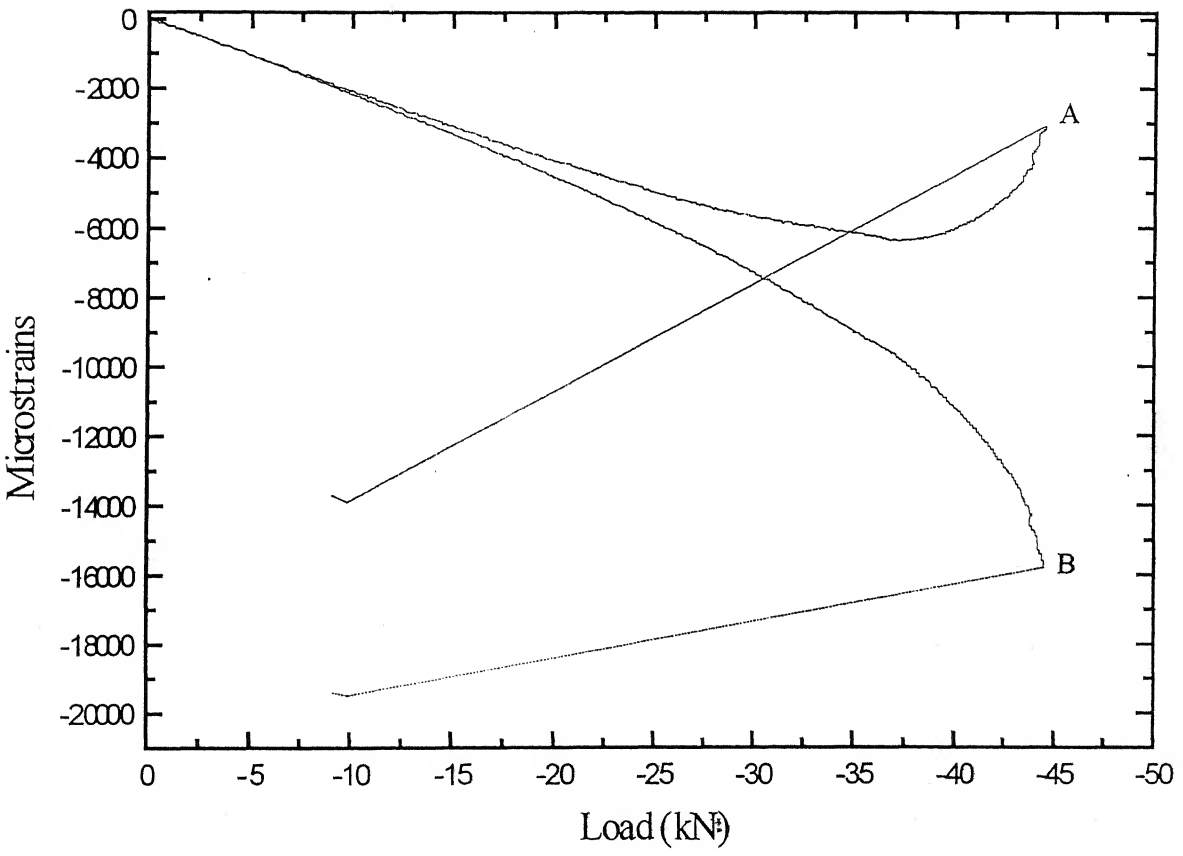

Fig. 4.5 Load verses strain curve for specimen B2

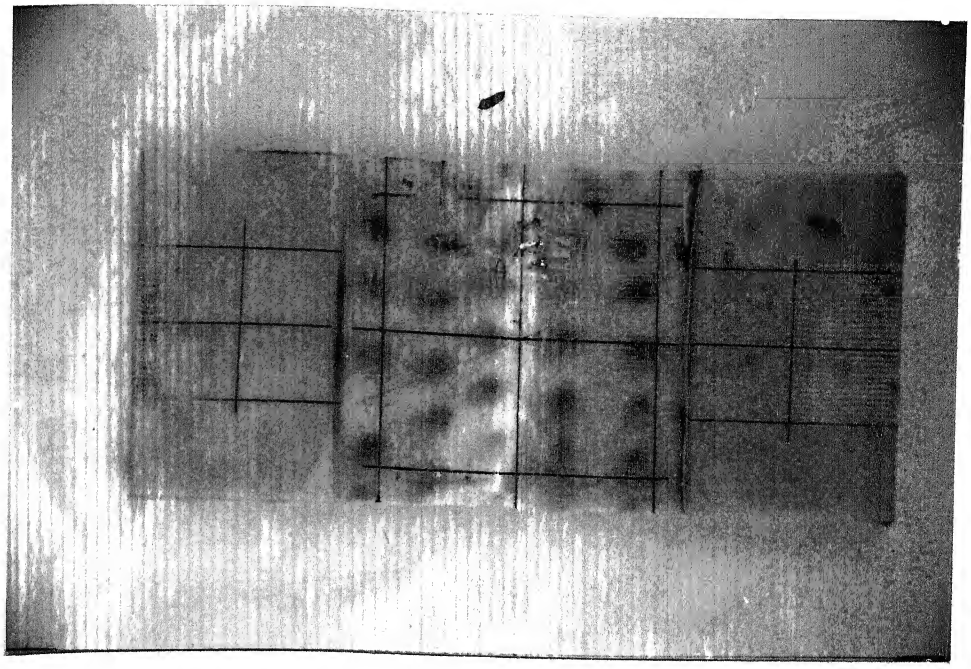

Fig. 4.6 Specimen B1 failed in compression test

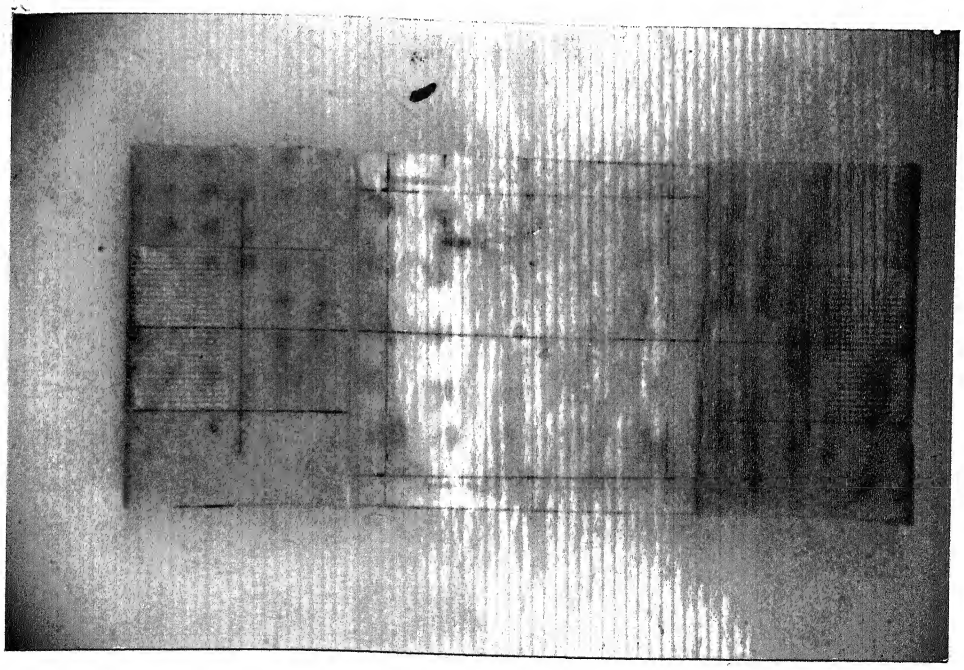

Fig 4.7 Specimen B2 failed in compression test

CHAPTER 5

CONCLUSIONS AND SUGGESTION FOR FUTURE WORK

5.1 CONCLUSIONS

A compression after impact (CAI) test facility is developed for FRP panels. For the impact test under controlled conditions an existing air gun test facility is instrumented and commissioned. An accurate velocity measurement system is developed, which uses the digital oscilloscope to display the time pulse for estimating the velocity of projectile. The accuracy in the time measurement from oscilloscope is in the error band of ± 0.5 μs, which is not very significant in comparison to the measured time more than 300 μs The accuracy of energy measurement is also within ± 0.5% (Appendix A1). The loss in the kinetic energy of projectile in reaching to the target is of the order of 0.05 Joule (Appendix A3). A compression test facility is also developed to avoid the buckling on the FRP panels. A buckling guide is designed to avoid the buckling of a panel during the compression test. The buckling guide is made of two rigid plates each having a rectangular hole of 80 mm^2 at the center. Each plate has a circumferential ridge whose top surface is ground flat. The buckling guide is suspended from the top and does not apply its dead weight on the specimen. A specially designed virtual instrumentation is developed for measuring the strains of strain gauges bonded on the panels. Two different kinds of specimens have tested to verify the proper working of developed experimental facilities. The results show that the developed experimental setup works well.

5.2 FUTURE SCOPE

⇒ Geometric, material and impact parameters should be optimized to obtain compressive failure through the growth of impact damage.

⇒ One can measure the lateral buckling using dial gauge or reverse engineering (a Fanoarm).

APPENDIX A1

Estimation of accuracy in energy measurement

The energy of the projectile impacting a FRP panel should be measured accurately to control the experiments. Thus, the velocity and mass of the projectile should be determined carefully. The projectile is weighed in an electronic balance, which measures the mass upto fourth decimal place of a gram. To measure the velocity of the projectile, as explained in Chapter 2, a laser light is cut by the projectile yielding a pulse. The velocity is thus determined by dividing the length of projectile by the duration of the pulse. Thus the kinetic energy of the projectile is given by

$$E = (½)\, m \times (L/T)^2 \quad \ldots\ldots \qquad (A1\text{-}1)$$

where, m is mass of projectile, L is length of projectile and T is duration of pulse
Differentiating equation A1-1 with respect to m, L and T one obtain

$$\Delta E = (½) \times [(L/T)^2 \times \Delta m + (2mL/T^2) \times \Delta l - (2mL^2/T^3) \times \Delta T\,] \quad .. \quad (A1\text{-}2)$$

Dividing equation A1-1 by equation A1-2 and realizing that error can be in positive or negative direction, one obtains

$$(\Delta E/E) = \pm (\Delta m/m) \pm 2(\Delta L/L) \pm 2(\Delta T/T) \quad \ldots\ldots \qquad (A1\text{-}3)$$

where, ΔE, Δm, ΔL, ΔT are the accuracy in measurement of energy, mass, length of projectile and duration for projectile respectively.

For a typical case for this study,

m = 7.5512 gm,	Δm = 0.0001 gm,
L = 22 mm;	ΔL = 0.02 mm,
T = 325 μs;	ΔT = 0.5 μs.

Equation A1-3 yields,

$$(\Delta E/E) = 0.004903$$
$$= 0.49\%$$

The accuracy is high enough; only the width of laser beam (1 mm diameter) controls the accuracy of measurement of energy. The error introduced is difficult to estimate but is of small order. The difficulty arises because of the fact that the front of geometry (spherical) of the projectile is different than the rear geometry (flat).

APPENDIX A2

Estimation of fall in height of projectile in reaching the target

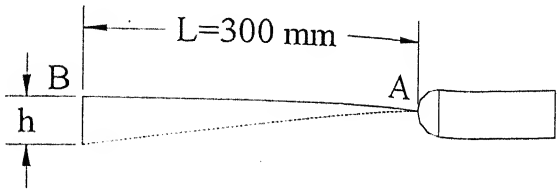

The target panel is placed at about L=300 mm from the barrel end and the projectile may fall during the free flight. In this appendix, the fall of the projectile is estimated. The projectile comes out from barrel at point A and hits the target at point B. The simple laws of motion gives the fall as

$$h = (½)\, gt^2, \quad \text{where } t = L/v$$

Thus, $$h = (½)g(L/v)^2$$

Considering a typical case of this study with

$L = 300$ mm

$v = 30$ m/s

The fall h turns out to be 0.49 mm which is not very significant. It is to be noted here that, whenever impact level is modified, the mass of the projectile is controlled such that projectile velocity is not less than 30 m/s.

APPENDIX A3

Estimation of drag and resulting loss of impact energy in between the point of measurement and point of impact

It has already been shown in Appendix A2 that target panel is placed at 300 mm far from the barrel end, whereas velocity of projectile is measured at the barrel end. The projectile has to travel in air till it reaches to target; the air drag may reduce the projectile velocity thus loss in the energy of projectile. One must estimate the air drag and loss of energy of projectile due to drag. This appendix shows the determination of air drag and loss of projectile energy. The drag force on the projectile is given as

$$\text{Drag force} = D = C_D \times (\rho V^2 A/2)$$

where, ρ is the density of air, V is velocity of projectile, A is cross-section of projectile, C_D is drag coefficient for projectile

The cross-sectional area of projectile is given as $(\pi/4)d^2$, thus drag force becomes

$$D = (C_D/2) \times (\rho V^2) \times \pi/4 \times d^2$$

For a typical case of this study

$$C_D = 0.6,\ \rho_{air} = 1.22,\ V = 50 \text{ m/s},\ d = 0.0126,$$

The drag force D turns out to be 0.114 N. Loss in energy of projectile is determined by the multiplication of drag force to the distance of target panel from the point of measurement of energy i.e. 300 mm. Thus, the loss in energy of projectile is comes out to be 0.0342 Joule, which is not very significant in comparison to the kinetic energy of projectile equal to 6 Joule.

REFERENCES

Broutman, L.J. and Rotem, A. (1973) "Impact strength and fracture of carbon fiber composite beams," *SPI, 28th Annual Technical Conference*, Washington, D.C, Section 17-B.

Broutman, L.J. and Rotem, A. (1975) "Impact strength and toughness of fiber composite material," in *Foreign Object Impact Damage to Composites*, ASTM STP 568, pp. 114 – 133.

Dorey, G., Sidey, G.R. and Hutchings, J. (1978) "Impact properties of carbon fiber/kevlar 49 fiber hybrid composites," *Composites*, vol. 9, pp. 25 – 32.

Mallick, P.K., and Broutman, L.J. (1975) "Impact properties of laminated angle ply composites," *SPI, 30th Annual technical conference*, Washington, D.C., Section 9 –C.

Agarwal, B.D. and Narang, J.N. (1977) "Strength and failure mechanism of anisotropic composites," *Fiber Science and Technology*, vol. 10 (1), pp. 37 – 52.

Tekeda, N., Sierakowski, R.L. and Malvern, L.E. (1982) "L.E.," *Experimental Mechanics*, vol. 22, pp. 20 - 5

Caprino, G. (1984) "Residual strength prediction of impacted CFRP laminates," *Journal of Composite Materials*, vol. 18, 508 –18

Liu, D. and Malvern, L.E. (1987) " Matrix cracking in impacted glass/epoxy plates," *Journal of Composite Materials*, vol. 21 (7), pp. 594 – 609.

Wyrick, D.A. and Adams, D.F. (1988) "Residual strength of a carbon/epoxy composite material subjected to repeated impact," *Journal of Composite Materials*, vol.22 (8), 749 – 765.

Kumar, P. and Narayanan, M.D. (1990) "Energy dissipation of projectile impacted panel of glass fabric reinforced composites," *Composite Structures*, vol. 15, pp. 75 –90, Elsevier Science Publisher Ltd., England.

Kumar, P. and Rai, B. (1991) "Reduction of impact damage in KFRP through replacement of surface plies with glass fabric plies," *Journal of Composite Materials*, vol. 25, pp. 694 – 702.

Kumar, P. and Rai, B. (1991) "Impact damage on single interface GFRP laminates – An experimental study," *Composite Structures*, Elsevier Science Publisher Ltd., England. vol. 18, pp. 1 - 10,

Kumar, P. and Singh, R.K. (2000) "Impact damage area and interlaminar toughness of modified FRP laminates," *Advanced Composite Materials*, vol. 9 (2), pp. 77 – 88.

Adanur, S., Xu, B. and Orak, H. (2000) "Braided composite automotive chassis frame," *International Community of Composite Engineering*, 7th International Annual Conference on Composite Engineering, Denver, Colorado, July 2-8, 2000, pp. 5 – 6.

Chao, C.C. and Chern, Y.C. (2000) "Three-dimensional nonlinear damage mechanics of composites," *International Community of Composite Engineering*, 7th International Annual Conference on Composite Engineering, Denver, Colorado, July 2-8, 2000, pp. B31 – B34.

Agarwal, B.D. and Broutman, L.J. (1990) "*Analysis and Performance of Fiber Composites*," Second Edition, John Wiley and Sons Inc.

Gupta, R.P. (1996) "Improvement in impact induced damaged area in FRP laminates," *M.Tech. Thesis*, Mechanical Engineering Department, IIT Kanpur.